

On the cause of a magnetospheric flux transfer event

Article

Published Version

Lockwood, M. ORCID: <https://orcid.org/0000-0002-7397-2172> and Hapgood, M. A. (1998) On the cause of a magnetospheric flux transfer event. *Journal of Geophysical Research*, 103 (A11). pp. 26453-26478. ISSN 0148-0227 doi: <https://doi.org/10.1029/98JA02244> Available at <https://centaur.reading.ac.uk/38756/>

It is advisable to refer to the publisher's version if you intend to cite from the work. See [Guidance on citing](#).

Published version at: <http://dx.doi.org/10.1029/98JA02244>

To link to this article DOI: <http://dx.doi.org/10.1029/98JA02244>

Publisher: American Geophysical Union

All outputs in CentAUR are protected by Intellectual Property Rights law, including copyright law. Copyright and IPR is retained by the creators or other copyright holders. Terms and conditions for use of this material are defined in the [End User Agreement](#).

www.reading.ac.uk/centaur

CentAUR

Central Archive at the University of Reading

Reading's research outputs online

On the cause of a magnetospheric flux transfer event

M. Lockwood and M. A. Hapgood

Rutherford Appleton Laboratory, Chilton, England, United Kingdom

Abstract. We present a detailed investigation of a magnetospheric flux transfer event (FTE) seen by the Active Magnetospheric Tracer Explorer (AMPTE) UKS and IRM satellites around 1046 UT on October 28, 1984. This event has been discussed many times previously in the literature and has been cited as support for a variety of theories of FTE formation. We make use of a model developed to reproduce ion precipitations seen in the cusp ionosphere. The analysis confirms that the FTE is well explained as a brief excursion into an open low-latitude boundary layer (LLBL), as predicted by two theories of magnetospheric FTEs, namely, that they are bulges in the open LLBL due to reconnection rate enhancements or that they are indentations of the magnetopause by magnetosheath pressure increases (but in the presence of ongoing steady reconnection). The indentation of the inner edge of the open LLBL that these two models seek to explain is found to be shallow for this event. The ion model reproduces the continuous evolution of the ion distribution function between the sheath-like population at the event center and the surrounding magnetospheric populations; it also provides an explanation of the high-pressure core of the event as comprising field lines that were reconnected considerably earlier than those that are draped over it to give the event boundary layer. The magnetopause transition parameter is used to isolate a field rotation on the boundaries of the core, which is subjected to the tangential stress balance test. The test identifies this to be a convecting structure, which is neither a rotational discontinuity (RD) nor a contact discontinuity, but could possibly be a slow shock. In addition, evidence for ion reflection off a weak RD on the magnetospheric side of this structure is found. The event structure is consistent in many ways with features predicted for the open LLBL by analytic MHD theories and by MHD and hybrid simulations. The de Hoffman-Teller velocity of the structure is significantly different from that of the magnetosheath flow, indicating that it is not an indentation caused by a high-pressure pulse in the sheath but is consistent with the motion of newly opened field lines (different from the sheath flow because of the magnetic tension force) deduced from the best fit to the ion data. However, we cannot here rule out the possibility that the sheath flow pattern has changed in the long interval between the two satellites observing the FTE and subsequently emerging into the magnetosheath; thus this test is not conclusive in this particular case. Analysis of the fitted elapsed time since reconnection shows that the core of the event was reconnected in one pulse and the event boundary layer was reconnected in a subsequent pulse. Between these two pulses is a period of very low (but nonzero) reconnection rate, which lasts about 14 mins. Thus the analysis supports, but does not definitively verify, the concept that the FTE is a partial passage into an open LLBL caused by a traveling bulge in that layer produced by a pulse in reconnection rate.

1. Flux Transfer Event Models

Flux transfer events (FTEs) were first identified in data from the dayside magnetopause, taken by the ISEE 1 and 2 [Russell and Elphic, 1978, 1979] and the HEOS 2 spacecraft [Haerendel *et al.*, 1978]. The key defining features of the events are a bipolar oscillation in the boundary normal component of the magnetic field (B_N) and a rise in the field strength at the event center. Studies using the nearby ISEE 1 and 2 craft suggested that the dimension of the FTEs normal to the magnetopause was typically of the order of $1 R_E$ (a mean Earth radius, $1 R_E = 6370$ km) [Saunders *et al.*, 1984 a, b]. Statistical surveys of the occurrence of these events showed that they are seen predominantly when the magnetosheath or interplanetary magnetic field points southward [Berchem and Russell, 1984; Rijnbeek *et al.*, 1984; Southwood *et al.*, 1986; Kuo *et al.*, 1995], strongly suggesting an association with magnetic reconnection.

However, seemingly similar events observed closer to the Earth, and so probably deeper in the magnetosphere, show little or no tendency to occur during southward interplanetary magnetic field (IMF) [Kawano *et al.*, 1992; Borodkova *et al.*, 1995; Sanny *et al.*, 1996]. Sibeck and Newell [1995] questioned the association of magnetospheric FTEs with southward IMF and magnetosheath field orientations, pointing out that if the sheath field was used, it was usually observed later/earlier in the same pass as the FTE and that the sheath field direction was likely to change in the intervening time. In addition, they pointed out that the spatial structure in the interplanetary medium can often result in the IMF orientation, as observed by an upstream satellite, differing from that of the magnetosheath field and that uncertainties in the propagation delay from the IMF monitor to the magnetopause could be important. However, none of these effects would bias the statistical surveys toward southward IMF conditions, and so they do not offer an explanation of the preponderance of southward IMF/sheath field during FTEs. Figures 1–4 illustrate four different models that have been proposed to explain FTE signatures at the magnetopause and their putative ionospheric signatures.

Copyright 1998 by the American Geophysical Union.

Paper number 98JA02244.
0148-0227/98/98JA-02244\$09.00

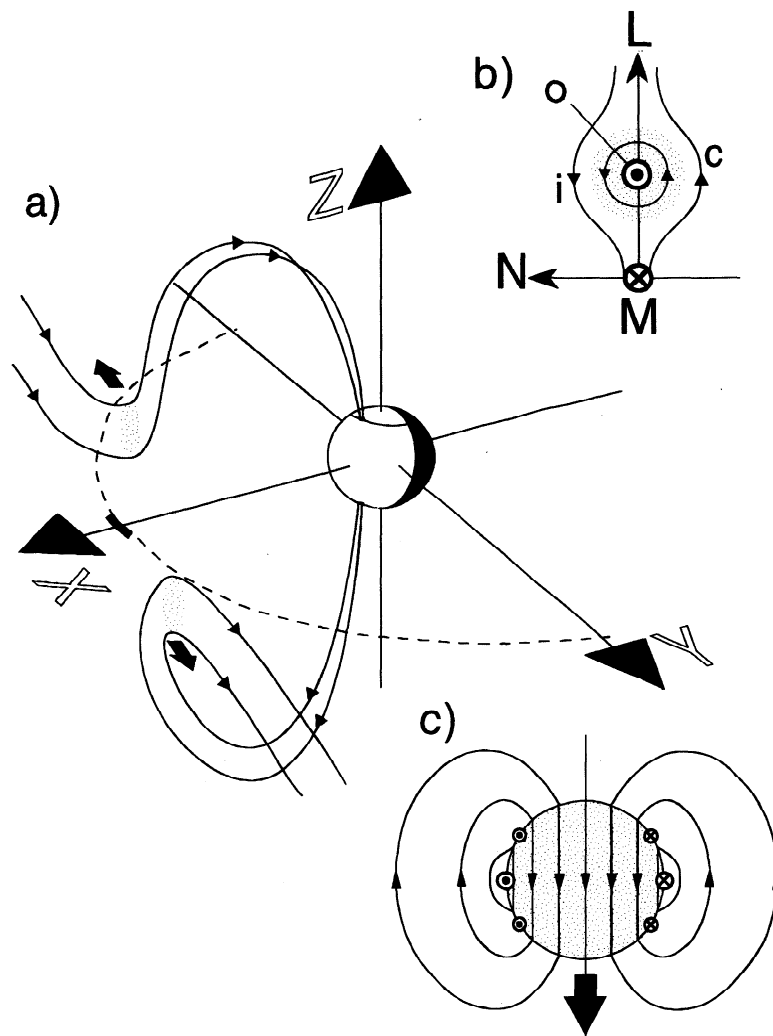


Figure 1. Schematic illustration of the fossil flux tube model of magnetopause flux transfer events (FTEs). (a) A view of the magnetosphere from the midlatitude and the midafternoon sector and in the GSM XYZ frame. The dashed line shows the equatorial magnetopause in which there is a short ($\sim 1 R_E$) reconnection X line shown by a heavy solid line. The newly opened field lines form an approximately circular flux tube (shown by the shaded cross section at the magnetopause), which evolves away from the reconnection site in the direction of the large arrow. The small arrows show the magnetic field direction. (b) A cross section of the magnetopause in boundary normal, LMN coordinates, showing interplanetary magnetosheath (i) and closed magnetospheric (c) field lines draped over the twisted open field lines (o) of the tube. (c) View looking down on the predicted ionospheric signature with flow streamlines and field aligned currents (out of the plane of the figure).

1.1. Flux Rope Model

Figure 1a shows the original FTE model proposed by *Russell and Elphic* [1978], which invokes a pulse of reconnection at a relatively short ($\sim 1 R_E$) reconnection X line, shown as the thick solid line in the equatorial magnetopause (dashed line). The newly opened flux tubes in the two hemispheres produced by this pulse are shown in the GSM (X,Y,Z) frame, viewed from northern middle latitudes in the midafternoon sector. Figure 1b shows a cross section of the magnetopause in boundary normal (L, M, N) coordinates. In the case shown, the newly opened flux (labeled o) is in the -M direction (i.e., roughly toward the dusk flank) and forms a bulge over which the interplanetary field lines of the magnetosheath (i) and closed field lines of the magnetosphere (c) are draped to give the bipolar signature in the boundary normal field, B_N . Inside the region of newly opened flux there is a bipolar signature because the field is twisted into

a helical form. As the flux tube in the northern hemisphere moves in the +L direction (northward in GSM), the field points outward ($B_N > 0$) and then inward ($B_N < 0$), giving a "standard polarity" FTE. The opposite sequence is seen in the southern hemisphere, where the event moves in the -L direction, giving a "reverse polarity" event. This is observed in statistical surveys of the occurrence of standard and reverse events [*Berchem and Russell*, 1984; *Rijnbeek et al.*, 1984] and is consistent with the sense of field aligned flow of escaping energetic magnetospheric plasma along the newly open field lines at the event center [*Daly et al.*, 1984]. The event polarity is the same on both sides of the magnetopause, as has been directly observed in "two-regime" events when observations were made simultaneously on the two sides of the magnetopause [*Farrugia et al.*, 1987b; *Lockwood*, 1991]. The draping of the field lines has been shown to be consistent with a bulge in the magnetopause [*Farrugia et al.*,

1987a; Walthour *et al.*, 1994]. The cores of FTEs, on both sides of the magnetopause, are observed to contain a mixture of plasmas of magnetospheric and magnetosheath origin [Thompson *et al.*, 1987; Klumpar *et al.*, 1990], consistent with the idea that they are newly reconnected field lines.

Figure 1c shows the predicted ionospheric signature for this FTE model (viewed looking down on the northern hemisphere footprint of the opened flux tube), as postulated by Goertz *et al.* [1985] and Southwood [1985; 1987]. The footprint of the newly opened flux tube moves as the field lines evolve from the reconnection site into the tail lobe under the joint action of magnetosheath flow and magnetic tension. The footprint has been assumed here to be circular, and while it is moving faster than the surrounding closed or open flux tubes (in the direction of the solid arrow), it would excite flow of the type shown by the streamlines. This calls for field aligned currents into and out of the ionosphere on the event edges, as shown. Many have tried to identify flow and current signatures of this kind [e.g., Goertz *et al.*, 1985; Todd *et al.*, 1986; Lockwood and Smith, 1989], but most attempts have been inconclusive, and many candidates are better explained by other models. Some potential cases have been shown to be traveling convection vortices (TCVs) [Lühr *et al.*, 1993] and/or events associated with solar wind pressure pulse effects [Sibeck *et al.*, 1989b; Sibeck and Croley, 1991] (see section 1.4). Other reported events are found to be elongated and evolving flow channels rather than circular moving flux tubes [Lockwood *et al.*, 1990; Pinnock *et al.*, 1993] (see section 1.2).

The evolution of newly opened flux tubes into the tail would correspond to a poleward motion in the ionosphere, and poleward moving events are indeed seen during southward IMF in the cusp aurora [e.g., Sandholt *et al.*, 1992]. These events have other properties (for example IMF B_y -dependent longitudinal motion and plasma flow in the event, which match the event phase motion [Lockwood *et al.*, 1989a, b, 1990]), which strongly associates them with patches of newly opened flux and reconnection pulses. An alternative explanation was proposed by Newell and Sibeck [1993a], who suggested that these events were caused by IMF or magnetosheath B_y changes during steady magnetopause reconnection; however, Lockwood *et al.* [1995b] showed that this explanation is inconsistent with the pattern of motion of the events. At the time of writing, only one set of measurements has compared magnetopause FTE observations with simultaneous observations of these poleward moving dayside cusp transients: Elphic *et al.* [1990] presented observation of a few magnetopause FTEs that occurred at the time of a few poleward moving cusp/cleft auroral events and associated ionospheric flow channels. The distribution of repeat periods of poleward moving cusp auroral transients [Fasel *et al.*, 1994] is very similar to that for magnetopause FTEs found by Lockwood and Wild [1993] and Kuo *et al.* [1995], the mode value being about 3 min and the average about 8 min in both cases.

In summary, the flux rope model invokes patchy and sporadic reconnection, which produces tubes of newly opened flux that are dragged over the satellite. It is inherently a three-dimensional model. It explains a great many of the reported features of magnetopause FTE signatures and their occurrence, as well as some of the features of cusp ionospheric transients.

1.2. Two-dimensional (2-D) Reconnection Pulse Model

Saunders [1983] and Southwood *et al.* [1988] pointed out that it is not necessary to use all three spatial dimensions to explain

magnetopause FTE signatures. This model is similar to the flux rope model in many ways, but it explains the bulge as the effect of a pulse of enhanced reconnection rate at an X line whose length is not specified. Such bulges can be reproduced in MHD simulations [Scholer, 1988a, b, 1989; Ma *et al.*, 1994] and in analytic theories of the reconnection layer during pulsed reconnection [Semenov *et al.*, 1991, 1992a, b; Rijnbeek *et al.*, 1991]. However, Scholer [1989] and Ku and Sibeck [1997, 1998] point out that in the two-dimensional MHD simulations the FTE signatures become more/less pronounced on the magnetosheath/magnetosphere side of the boundary as the ratio of the sheath to magnetosphere field strengths (B_{sh}/B_{sp}) decreases, to the extent that magnetospheric FTE signatures vanish for (B_{sh}/B_{sp}) less than about 0.5. This effect may well be due to the two-dimensional nature of these simulations. Southwood *et al.* [1988] noted the effect of adding the third dimension: shear across the magnetopause, either in the field (skew) or in the flow in the third dimension, will cause helical twist of the field in the FTE core, giving an excess pressure. A lack of magnetospheric FTEs can also be found in analytic MHD calculations, but only for some two-dimensional cases; if the fields on the two sides of the boundary are skewed and/or the flow is sheared, the analytic calculations do reveal magnetospheric FTEs [Semenov *et al.*, 1992b; V. Semenov, private communication, 1998]. Another difference pointed out by Ding *et al.* [1991] and Ku and Sibeck [1997] is that two-dimensional MHD models often produce highly asymmetric, almost monopolar variations in B_N , as opposed to the more symmetric events often selected for presentation in the literature (including the example studied in the present paper).

Figure 2 illustrates this model in the same format as Figure 1. In Figure 2b the newly opened field has no component in the M direction, unlike that in Figure 1b. Such a component can be added and effectively gives the twist to the event [Southwood *et al.*, 1988]. The event can be cylindrically extended in the direction normal to its motion as in Figure 2a. Unless the flow streamlines tangential to the magnetopause change, the satellite will see only those field lines that were reconnected at one point of the X line, and thus there is no information about the extent of the event or of the X line. Newell and Sibeck [1993b] argued that this extent, and hence the total FTE contribution to the total transpolar voltage, is limited. However, Lockwood *et al.* [1995a] disagreed with the principle of these limits, as they were based on the concept that all of each event (over its entire longitudinal extent) must be reconnected in an interval about 2 min long (as opposed to the reconnection lasting about 2 min each longitude, as invoked to explain the poleward moving transients [Lockwood *et al.*, 1993c]). Lockwood *et al.* [1995a] also pointed out that if events are not longitudinally extensive, then there must simultaneously be many of them at different local times to explain the high observed occurrence probabilities at the different local times; this explanation means that the total voltage contribution of FTEs, collectively, is independent of their individual extent.

A big advantage of this model over the fossil flux tube model is that the draped field lines coating the event can map back to a reconnection X line that is still active. Thus, for example, it offers an explanation of counterstreaming electrons on the FTE borders [Scholer *et al.*, 1982; Southwood *et al.*, 1988]. Bryant and Riggs [1989] and Hapgood and Lockwood [1995] have noted that the electron and ion characteristics in FTEs have a structure like that seen in the LLBL during most other magnetopause crossings. By comparing data from the Active Magnetospheric Trace Explorer (AMPTe) UKS and IRM

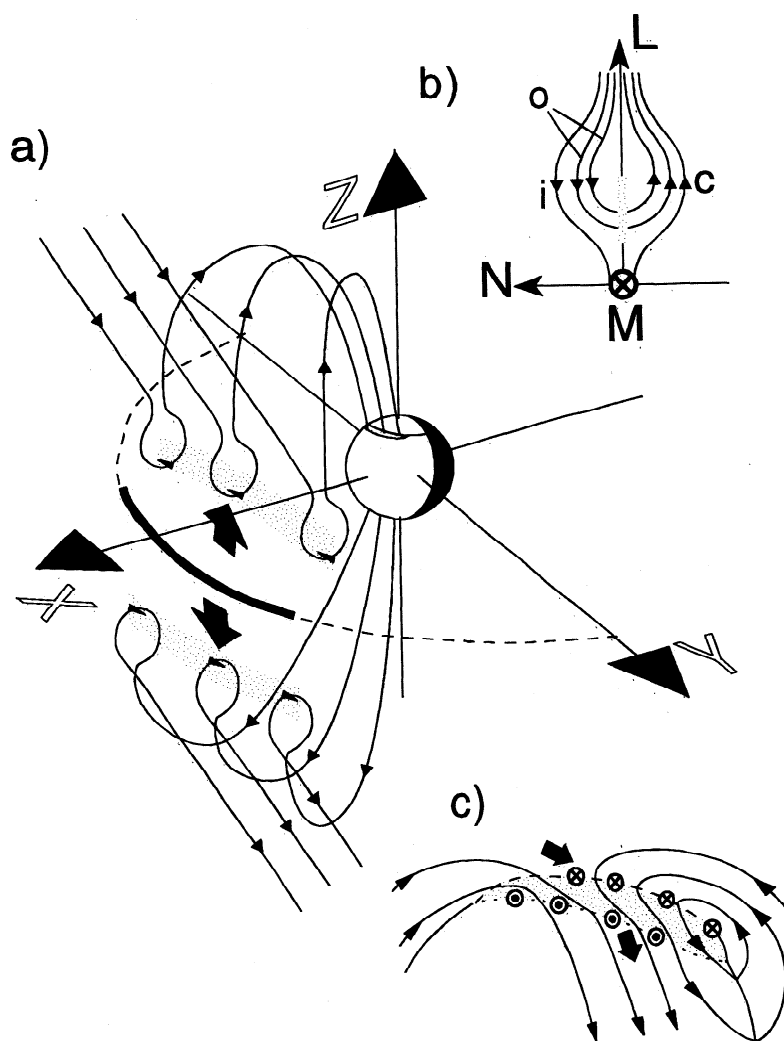


Figure 2. Two-dimensional cylindrically symmetric reconnection pulse model, shown in the same format as Figure 1. The longitudinal extent of the X line and of the FTE events is not specified.

satellites, *Hapgood and Lockwood* [1995] found that FTE's were transient thickenings of the LLBL, consistent with this model. The model also predicts that accelerated flows should be seen on the trailing edge of many FTE events [*Lockwood and Smith*, 1994], as has been observed [*Paschmann et al.*, 1982].

Figure 2c shows the signatures of these events in the ionosphere, as predicted by *Cowley et al.* [1991], *Lockwood et al.* [1993c], and *Lockwood* [1994]. In principle, this signature is the same as that for the flux rope model, but it allows for longitudinal event elongation and the fact that event shape and motion evolve as newly opened flux is appended to the tail lobe. A key and unique prediction of this model is that patches of newly opened flux, produced by successive reconnection pulses, are appended to each other in a contiguous manner, causing discontinuous steps in the cusp ion dispersion on the boundaries between poleward moving events. The observation of these "cusp ion steps" in association with poleward moving events [*Lockwood et al.*, 1993b; *Pinnock et al.*, 1995] is therefore very strong support for this model of FTE signature, and the ions' dispersion is direct evidence that the reconnection rate is indeed pulsed [*Lockwood and Smith*, 1992; *Lockwood et al.*, 1995c; *Lockwood and Davis*, 1996a, b]. That the longitudinal extent of

these events can be large is shown by the extended flow channels [*Lockwood et al.*, 1990; 1993a; *Pinnock et al.*, 1993] and by longitudinal satellite passes showing coherent stepped ion dispersion features [*Lockwood and Davis*, 1996b].

The two-dimensional reconnection pulse is similar in many ways to the flux rope model from which it evolved. Indeed, if the reconnection X line is short, this model can re-produce the "elbow" of newly opened field lines of the fossil flux tube model [*Semenov et al.*, 1995]. As a result the two-dimensional model shares many of the fossil flux tube model's successes but has some additional advantages in terms of explaining the magnetopause FTE signatures. In addition, it has been very successful in both explaining and predicting observed ionospheric signatures in the cusp region (such as extended flow channels and cusp ion steps).

1.3. Multiple X line Model

Figure 3 illustrates the multiple X line model proposed by *Lee and Fu* [1985], which invokes twisted field lines between multiple reconnection sites. By invoking reconnection this model, like the two FTE models discussed above, can explain

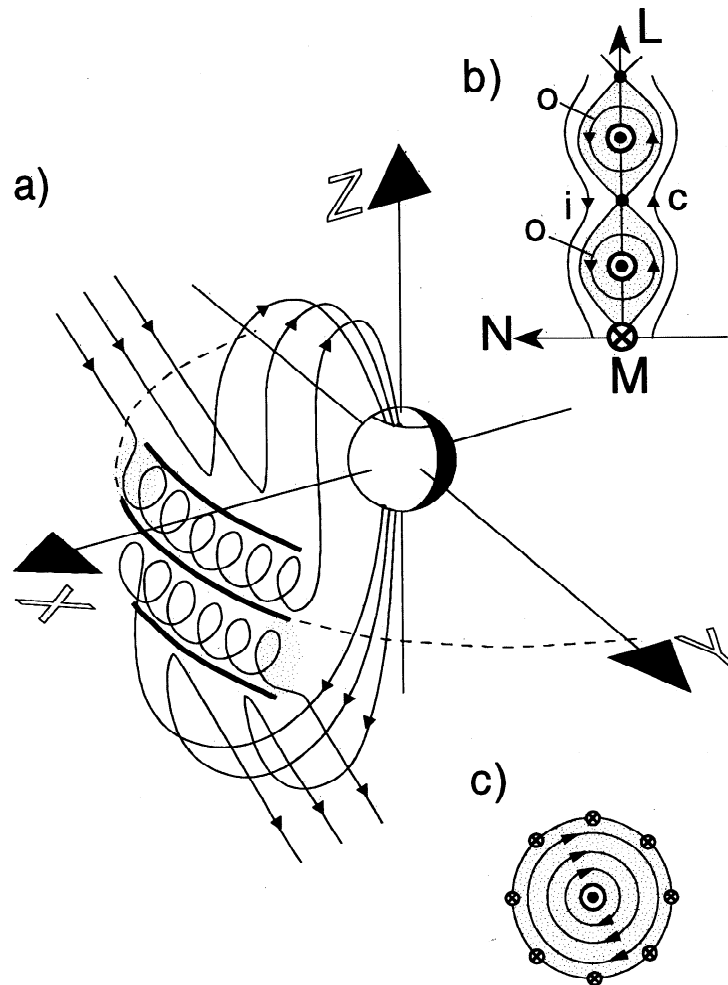


Figure 3. Multiple reconnection X line model, shown in the same format as Figure 1.

the dependence of the occurrence on IMF B_z , the mixing of magnetosheath and magnetosphere plasma inside FTEs, and the field twist there [Liu *et al.*, 1992; Shi *et al.*, 1991]. However, it cannot explain the accelerated flows seen on the trailing edge of some FTEs, as this flow is formed by the evolution of field lines away from a single reconnection site [Ma *et al.*, 1994]. As for the cylindrical 2-D model, the extension of the reconnection sites over large longitudinal distances can explain the large occurrence frequency of events at all local times [Rijnbeek *et al.*, 1984; Lockwood *et al.*, 1995a], as shown in Figure 3a. To give the bipolar B_N signatures, both the X lines and the bulges between them (shown in Figure 3b) must evolve away from low latitudes over the satellite. This effect would give a continuous string of B_N oscillations (" B_N activity") rather than the isolated events with a wide range of separations between 2 and 20 min [Lockwood and Wild, 1993; Kuo *et al.*, 1995]. Examples of such B_N activity are not difficult to find [e.g., Elphic and Southwood, 1987; Elphic *et al.*, 1990] and may well be explained as multiple X lines: however, this remains an unsatisfactory explanation of isolated FTE events.

Lee [1986] envisaged the twisted flux tubes untwisting and generating ionospheric signatures like the one shown in Figure 3c, with a coaxial field aligned current structure. If such an untwisting flux tube drifts over a ground station, it will generate a mixture of the signatures shown in Figures 1c and 3c

[Lockwood *et al.*, 1990]. Such signatures have been reported, but generally as part of a twin vortex (TCV), as discussed below in section 1.4. It has also been suggested that the multiple X lines are linked to observed multiple brightenings of dayside auroral transients [Fasel *et al.*, 1993].

1.4. Magnetosheath Pressure Pulse Model

The only properly formulated model of FTE signatures that does not directly invoke reconnection is that by Sibeck [1990; 1992]. This model was discussed specifically in relation to the FTE event that is the subject of the present paper. In its original form a pressure pulse in the magnetosheath was envisaged to produce a traveling indentation of the magnetopause, which moves the magnetopause over the satellite so that the satellite briefly enters the plasma depletion layer (PDL) during northward sheath field. However, a serious objection to the model, as originally posed, was that the distribution function at the center of the event is not like that expected for the PDL [Smith and Owen, 1992]. Although distribution functions in the PDL are not available for the time of this FTE, on other passes they are significantly different [Fuselier *et al.*, 1991, 1995] and as predicted by Cowley [1982]. Smith and Owen found a D-shaped distribution at the event core, as was predicted for an open LLBL by Cowley. These distributions are seen in data from

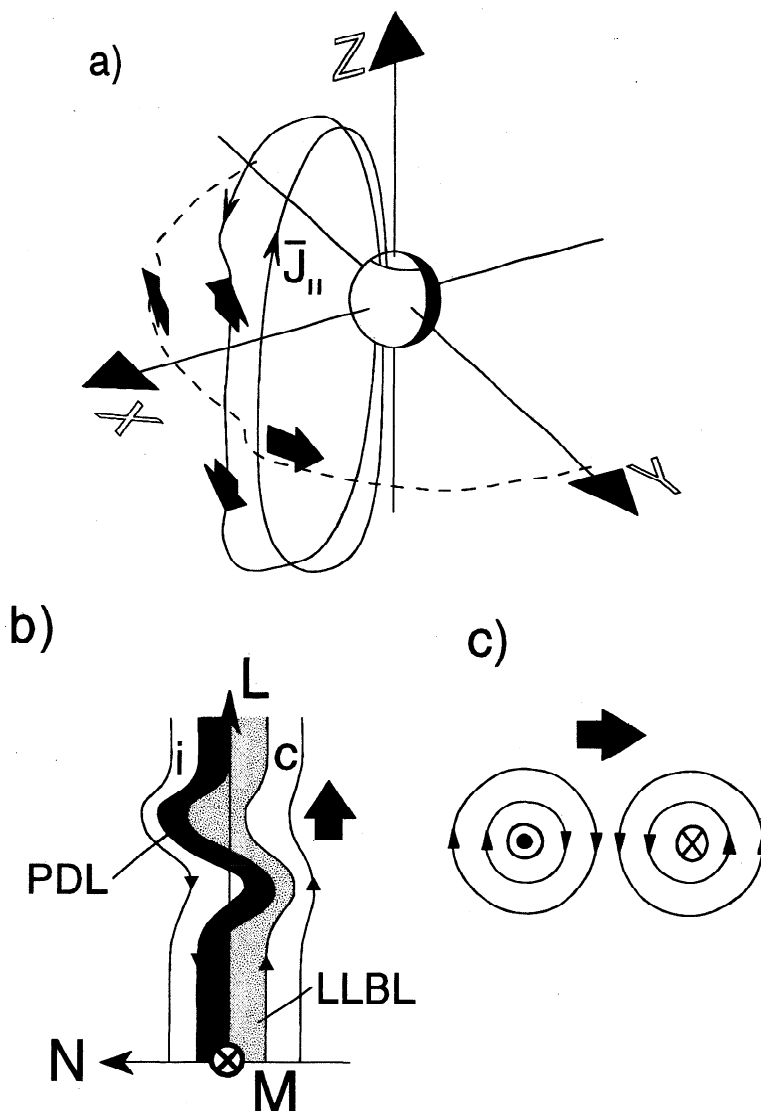


Figure 4. Magnetosheath pressure pulse model, shown in the same format as Figure 1.

the LLBL [Gosling *et al.*, 1990a]; furthermore, Fuselier *et al.* [1991] reported a case study in which all populations (of magnetosheath and magnetospheric origin on both sides of the boundary) were as predicted by Cowley, a result which has been found to hold true in other cases [Fuselier *et al.*, 1995]. Smith and Rodgers [1991] showed that the low-velocity cutoff of the D-shaped distribution is close to the de Hoffman-Teller velocity [de Hoffman and Teller, 1950], as is required by the theory. Gosling *et al.* [1990b] showed that these distributions were found in the expected location, relative to the ion and electron edges for an open LLBL.

The distribution function at the event center found by Smith and Owen [1992] therefore indicates that the pressure pulse FTE model must be amended somewhat, in that the satellite must enter an open LLBL at the event center instead of crossing the magnetopause into the PDL. Such a possibility was indeed mentioned for this event by Sibeck [1990]. Therefore reconnection must be ongoing at the time of the pressure pulse impact. This explanation is more satisfactory in other respects. For example, the original version of the model required all magnetospheric FTEs in which the core is intersected to take place during northward magnetosheath field, because the field in

the core of magnetospheric FTEs, where sheath-like plasma is seen, is always northward. Thus, if the satellite entered the PDL in the event core, the sheath field would have been northward, inconsistent with the observation occurrence statistics, which show that magnetospheric FTEs tend to occur during southward IMF/sheath field [Rijnbeek *et al.*, 1984; Berchem and Russell, 1984; Kuo *et al.*, 1995].

The ionospheric signature predicted for this kind of event is shown in Figure 4c. The traveling indentation of the magnetopause generates a pair of field aligned currents [Kivelson and Southwood, 1991], which produce a pair of TCVs [Friis-Christiansen *et al.*, 1988; Glatfmeier *et al.*, 1989; Glatfmeier, 1992]. Note that there is a difference between the theories of Kivelson and Southwood [1991] and Glatfmeier [1992]: in the former the pair of field aligned currents are generated by a single change in magnetopause position, whereas the latter predicts that they are caused by an in-out or out-in motion of the boundary. There is no doubt that some events thought to be the vortical footprints of isolated reconnected flux tubes were in fact TCVs driven by solar wind dynamic pressure variations (for example, the case discussed by Todd *et al.* [1986]; Sibeck *et al.* [1989b], and Lühr *et al.* [1993]). A key test for TCVs is that the direction of flow at the event

center is not the same as the phase motion of the event as a whole (as in Figure 4c), whereas it is the same for a reconnected flux tube (as in Figures 1c and 2c). This test shows that the elongated poleward moving auroral transients are consistent with reconnected flux tubes (as in Figure 2c) [Lockwood *et al.*, 1990, 1993a] but that other events are consistent with TCVs [Friis-Christiansen *et al.*, 1988]. Farrugia *et al.* [1989] demonstrated a TCV signature associated with solar wind dynamic pressure pulse and magnetopause boundary motions. Furthermore, there are transient cusp aurorae associated with TCVs [e.g., Lühr *et al.*, 1996], but these are different in character from the poleward moving transients seen detaching from the poleward edge of the cusp aurora: they move longitudinally equatorward of the cusp [Jacobsen *et al.*, 1991].

The pressure pulse model has been the source of considerable debate [e.g., Elphic, 1990; Song *et al.*, 1994; Sibeck and Newell, 1995]. Elphic *et al.* [1994] surveyed simultaneous magnetosheath data during magnetospheric FTE events, using combined data from the AMPTE and ISEE satellites. They found no pressure pulse triggers for the FTEs, indeed no triggers of any kind, in the magnetosheath. On the other hand, Sibeck [1990] related FTE signatures to foreshock pressure variations, and Sibeck [1994] related them to pressure pulses in the sheath. There may be a number of reasons these studies produced these two contradictory conclusions. First, there may have been uncertainties in the density data employed by Elphic *et al.* [Sibeck, 1992]; second, Sibeck allowed the lag between the magnetosheath and magnetopause observations to have some variations, which would smear out any pressure pulses in the superposed epoch study employed by Elphic *et al.*

Lockwood [1991] pointed out that the pressure pulse model has great difficulty in explaining "two-regime" events (events observed by two craft simultaneously on opposite sides of the magnetopause [Farrugia *et al.*, 1987b]), particularly without invoking tripolar, rather than bipolar, B_N signatures. However, the amended pressure pulse model can explain magnetospheric FTE signatures on a case-by-case basis. Indeed, it is very difficult to determine whether a temporary passage of a lone satellite into the open LLBL is caused by an indentation of the reconnecting magnetopause due to a magnetosheath pressure pulse, or whether the boundary layer has grown in thickness in response to a reconnection rate pulse.

2. Previous Studies of the October 28, 1984, Event

The FTE studied here has been the subject of many previous studies. It was observed by the AMPTE UKS and IRM satellites around 1046 UT on October 28, 1984, on an outbound magnetopause crossing. The satellites were at a GSM latitude of 25.7° (northern hemisphere) and at a magnetic local time of 08:55 (i.e., in the midmorning sector). They were separated by 180 km in a direction roughly aligned with the boundary normal (as determined from the magnetopause crossing by UKS, which took place considerably later, at 1145–1245 UT), with UKS closer to the boundary than IRM. This event was first reported by Rijnbeek *et al.* [1987], who noted its layered structure. Subsequently, it has been the subject of studies by Farrugia *et al.* [1988], Lockwood *et al.*, [1988], Bryant and Riggs [1989], Sibeck [1992], Sibeck and Smith [1992], Smith and Owen [1992], and Lockwood and Hapgood [1997]. Rijnbeek *et al.* [1987] and Farrugia *et al.* [1988] showed that there was a high-pressure core at the event center predominantly due to particle pressure, but that outside this was a layer of high magnetic pressure and low particle pressure. The origin of this high-

pressure core has never been satisfactorily explained. Sibeck and Smith [1992] analyzed the flows around this event and could not fit them satisfactorily to any of the above models. The flows were particularly strange [cf. Smith *et al.*, 1987] on the trailing edge of the event, where Lockwood *et al.* [1988] noted large fluxes of upwelling ionospheric plasma. Thus despite the many studies of this event, many important facets have not been satisfactorily explained.

One reason this event has received so much attention is that it is one of the most clear-cut in the AMPTE data set, giving unprecedented resolution of field and particle data from two adjacent craft. It is also an archetypal "crater" event in terms of the magnetic field structure, showing the field characteristics that all the models aim to explain. However, in other respects this is a rather extraordinary event, when one considers that the satellites were at a latitude of only 25° yet at a magnetic local time (MLT) of 9 hours. One might have expected the tension force on the newly opened field lines to carry them to higher latitudes at this MLT, if they were reconnected close to the subsolar point. Thus if the event is caused by the passage of newly opened field lines (as proposed by three of the four FTE models), the location at which they were reconnected and their subsequent evolution need explanation. In this paper we gain some insight by studying the distance between the reconnection site and the satellites and the time elapsed since the flux tubes observed in the event were reconnected.

However, the main reason this event has been so controversial is that it was the basis of pressure pulse model shown in Figure 4 [Sibeck, 1990, 1992]. As we discussed above, Smith and Owen [1992] showed that the ion anisotropy in the event was inconsistent with a partial entry into the PDL, and indeed the ion distribution function in the event core was a D-shaped distribution, as predicted by Cowley [1982] for magnetosheath plasma injection along newly opened field lines. From an analysis of the variation of electron density and temperature in this event, Bryant and Riggs [1989] noted that the event appeared to have the same structure as that of the magnetopause crossing seen later in the pass. Recently, Lockwood and Hapgood [1997] have shown that both the ion and electron characteristics of this event can be explained as a temporary entry of the satellite into an open LLBL, confirming Smith and Owen's [1992] conclusion. However, as we discussed above, Sibeck's original concept can readily be adapted to allow for this conclusion, by simply allowing ongoing reconnection elsewhere on the magnetopause and identifying the event center with the open LLBL and not the magnetosheath PDL. With this modification of the pressure pulse model it joins the fossil flux rope model and the two-dimensional reconnection pulse model as being capable of explaining the ion distribution function at the center of this event, as observed by Smith and Owen [1992]. However, the magnetic islands produced by multiple X lines are not consistent with the theory of how such distributions are generated [see Lin and Lee, 1993a, b]. In addition, the simulations by Ma *et al.* [1994] show that fast flows along the magnetopause are not predicted in and around the magnetic islands between the X lines yet they are observed in this event [Sibeck and Smith, 1992]. Therefore the multiple X line model is not here considered further as a cause of this event.

3. Ion Model

Models of ion behavior in the magnetosphere have been developed and successfully used to predict signatures of ion precipitation into the cusp ionosphere [Onsager *et al.*, 1993; Onsager, 1994; Lockwood and Smith, 1994; Lockwood, 1995;

Lockwood and Davis, 1996b; Lockwood *et al.*, 1998]. These models include four main elements: (1) spatial variations of the magnetosheath density and temperature (to date, gasdynamic predictions have been employed [Spreiter *et al.*, 1966]); (2) the evolution of reconnected field lines over the magnetopause, as predicted by Cowley and Owen [1989]; (3) the theory of ion acceleration at the magnetopause current sheet by Cowley [1982]; (4) the time-of-flight velocity filter effect of ion motion along convecting field lines [Rosenbauer *et al.*, 1975; Reiff *et al.*, 1977]. These models have been very successful in reproducing cusp ion precipitation characteristics seen at both low and middle altitudes both during steady state conditions [Onsager *et al.*, 1993; Lockwood, 1997, respectively] or during pulsed reconnection [Lockwood and Davis, 1996b; Lockwood *et al.*, 1997, respectively].

An addition to the model of Cowley [1982] has been introduced by Lockwood *et al.* [1996], who allowed for reflection of magnetospheric ions off the Alfvén wave (hereafter called a rotational discontinuity, or RD) on the interior edge of the open LLBL, as well as at the main RD (i.e., the magnetopause itself) on the LLBL's outer edge. With this addition they were able to model energetic ion precipitation at the equatorward edge of the cusp dispersion ramp, generating the spectra as well as the moments of the ion distribution. The model, with this extension, was also successfully employed by Lockwood [1997] and Lockwood and Moen [1996] to match observed ion precipitation fluxes.

The time-dependent version of the model computes the ion spectrum seen at a given distance from the reconnection X line as a function of the time elapsed since reconnection, $(t_s - t_o)$, where t_s is the time at which a field line is observed and t_o is the time at which it was reconnected. This model can be used to compute the variation of the field aligned ion spectrum expected in this FTE signature, for the three models shown in Figures 1, 2, and 4. To do this, we require as inputs the ion distribution functions in the closed magnetosphere and in the magnetosheath. The magnetosphere population was directly observed outside the event by Smith and Owen [1992], but the magnetosheath population is here inferred from the LLBL distribution seen at the event center. The Cowley [1982] theory predicts that this injected population is the sheath population, truncated at a field parallel velocity cutoff (which in this case is close to zero) and with density reduced by the transmission factor $(1-r)$; thus we can use this theory to reconstruct the sheath population. We adopt the magnetopause reflection (r) and heating factors, which gave the best fits to the observed cusp precipitation studied by Lockwood *et al.* [1996]. The model also requires the field line velocity V_f as a function of $(t_s - t_o)$. We allow for the acceleration of the newly opened field lines away from the reconnection site, as derived in the next section.

In the case of the two-dimensional reconnection model and the (modified) pressure pulse model, a magnetospheric FTE would be described by simple continuous variations of $(t_s - t_o)$ as the boundary layer expands or is pushed over the satellite, respectively. The elapsed time since reconnection $(t_s - t_o)$ would initially have negative values (i.e., the satellite is on closed field lines in the magnetosphere that will be opened sometime in the future), which would increase to zero as the magnetic separatrix is approached and would equal zero at the moment the magnetic separatrix passed over the satellite. The satellite is then immersed deeper into the reconnection layer so $(t_s - t_o)$ increases, as discussed by Lockwood and Hapgood [1997]. Note that no changes can be seen until $(t_s - t_o)$ has a nonzero, positive value as

information and particles that result from the change in magnetic topology take a nonzero time to propagate from the reconnection site to the satellite. Thus the variation of $(t_s - t_o)$ at small and negative values does not influence the event. The reverse sequence is seen as the satellite exits from the event. Thus, for these models a continuous variation of $(t_s - t_o)$ of the kind shown by curve (1) in the top panel of Figure 5 applies.

On the other hand, the fossil flux tube model is described by a variation in $(t_s - t_o)$ like that shown in curve (2). In this case, $(t_s - t_o)$ changes discontinuously from negative to positive values as it enters the reconnected flux tube. It is here assumed that the reconnection pulse that forms the tube is shorter than the time taken for it to be dragged over the satellite and thus $(t_s - t_o)$ increases slightly as the event passes. When the satellite leaves the event, there is a discontinuous drop in $(t_s - t_o)$ back to negative values.

Parts b and c of Figure 5 show predicted energy-time ion spectrograms of differential energy flux of field aligned ions for these model variations of $(t_s - t_o)$, for a satellite located a field aligned distance of $6 R_E$ from the reconnection site. Figure 5b shows the predicted variation for the continuous change in $(t_s - t_o)$ predicted for the 2-D reconnection pulse and pressure pulse models (case 1 in Figure 5a). The first indication that the satellite has moved onto open field lines is the presence of enhanced fluxes at the highest energies. These are magnetospheric particles reflected off the interior RD. They cease abruptly as the interior RD passes over the satellite, and subsequently, magnetospheric ions reflected off the exterior RD (the magnetopause) are seen at the highest energies until these decay as the source magnetospheric population is lost. The fluxes of sheath ions increase but then fall again after $(t_s - t_o)$ peaks. The fluxes of sheath ions at the highest energy rise with $(t_s - t_o)$ in the event core because the field lines accelerate as they evolve away from the X line. A general property of newly reconnected field lines is a "cutoff" ion energy: at energies above this cutoff are ions that either are of magnetosheath origin and have been transmitted through the magnetopause or are of magnetospheric origin and have been reflected off one of the RDs; at energies below this cutoff are magnetospheric ions whose flight time from the reconnection site to the satellite is long enough for them to have not yet been affected by the change in field topology. This time-of-flight cut off energy is clearly seen in Figure 5b and decreases as $(t_s - t_o)$ increases. Note that this sequence is identical in principle to that seen by a low-altitude satellite flying poleward through the LLBL and into the low-latitude part of the cusp. At the magnetopause the reverse sequence is seen on leaving the event.

Figure 5c shows the corresponding sequence for curve (2) which simulates the fossil flux tube model. The key difference is that all field lines in the flux tube were opened in the short reconnection pulse and the event is draped with closed magnetospheric field lines. Thus the edges of the reconnected flux tube are marked by discontinuous changes in the ion spectrum, corresponding to the discontinuous steps in $(t_s - t_o)$.

It is now useful to study the ion spectrogram observed for the FTE event considered here, as presented here in Figure 5d and in the top panel of Plate 1 of Farrugia *et al.* [1988], showing the count rate (proportional to the differential energy flux) for all pitch angles and as a function of energy and time. The general similarity with Figure 5b is clear. Note that the predicted spectrogram in Figure 5b is not a fit to the observed one (Figure 5d), as it is based on arbitrary model inputs. A fit is explored in the next section. Most important, the observed ion spectrum

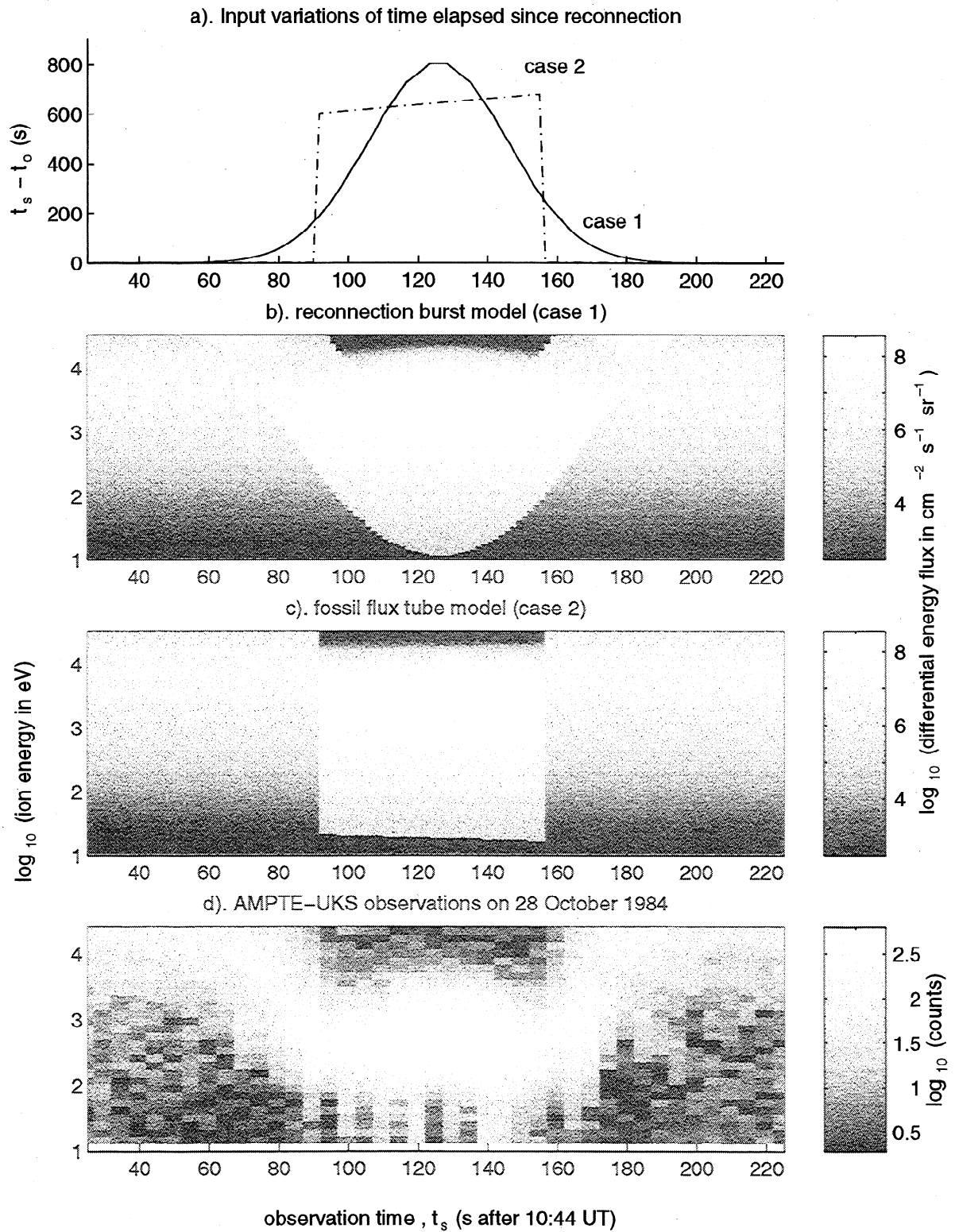


Figure 5. Predictions of the variations of the ion spectrum for the pulsed reconnection and fossil flux tube models (a). Input variations of elapsed time since reconnection ($t_s - t_0$) with observation time t_s , and the resultant ion energy-time ($E-t_s$) spectrograms of differential energy flux (proportional to the count rates plotted for the FTE event in Plate 1 of *Farrugia et al.* [1988]) for (b) the pulsed reconnection model and (c) the fossil flux tube model. The observations by AMPTE UKS in the October 4, 1984, event are shown in (d).

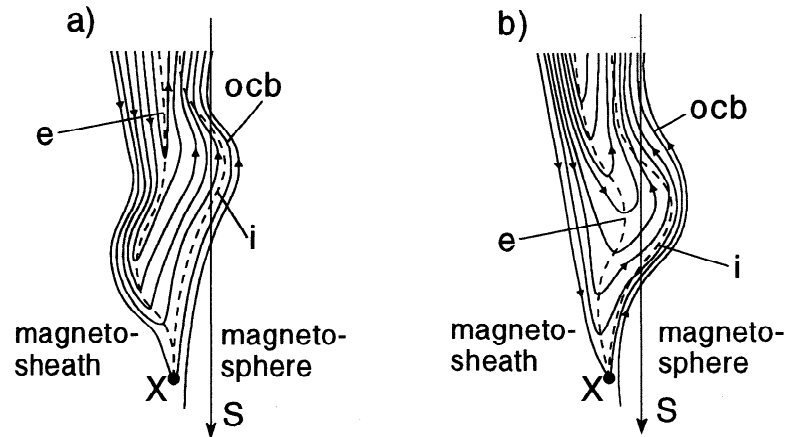


Figure 6. Explanations of the FTE event in terms of (a) the two-dimensional pulse model and (b) the pressure pulse model. X is the reconnection site; S is the satellite locus in the event rest frame; e and i are the rotational discontinuities (RDs) standing on the inflow on the magnetosheath and magnetosphere sides, respectively; and ocb is the open-closed field line boundary.

evolves continuously from sphere-like to sheath-like, which Figure 5 predicts for the 2-D reconnection pulse and the pressure pulse models. However, this behavior is not true for the fossil flux tube model. It would therefore be necessary to invoke some kind of additional boundary process to cause this evolution in the fossil flux tube model. In the absence of a viable proposal for such a mechanism we do not consider this model further here.

Figure 5b should also be compared with the ion spectrogram presented in Figure 9 of *Bryant and Riggs* [1989]. This spectrogram is for a magnetopause crossing but has been reordered to be in energy-transition parameter (E - τ) format instead of the usual energy-observation time (E - t_o) format. The transition parameter is discussed in section 5 of the present paper. The similarities are striking, with the same evolution from sheath-like to sphere-like ion populations observed. Thus the ion model can reproduce the spectral variations of the ions in both FTEs and magnetopause crossings. Added to the conclusion of *Bryant and Riggs* [1989] and *Lockwood and Hapgood* [1997] that the electron characteristics of the FTE and the boundary layer are essentially the same, this finding supports the idea that the FTE is a partial crossing of the (open) magnetopause LBL. Thus we conclude that this FTE has one of two causes, illustrated here in Figure 6.

Figure 6a shows the reconnection pulse model, in which a bulge in the reconnection layer (i.e., the open LBL) is formed by an excess pressure in the reconnection layer, caused by a pulse of enhanced reconnection rate at the X line, X. The arrow labeled S is the effective trajectory of the AMPTE UKS satellite in the rest frame of the disturbance on the magnetospheric side of the boundary. The perturbation moves faster on the magnetosphere side, as the Alfvén speed is greater there than on the sheath side. The bulge on the magnetospheric side moves the open-closed boundary (ocb) and the interior RD (i) over the satellite, so that it is briefly in the open LBL. At the center of the event, the satellite sees field lines that were reconnected earlier than those seen on both edges of the event; i.e., elapsed time since reconnection ($t_s - t_o$) increases towards the event center. Figure 6b shows the alternative explanation in terms of the pressure pulse model. Here the traveling bulges in ocb and i are caused by a similar indentation in the exterior RD (e), i.e.,

the main magnetopause current layer. This indentation is caused by high pressure in the magnetosheath. To fit the ion observations, ongoing reconnection must be taking place at X and, as for the reconnection pulse model, i.e., elapsed time since reconnection, ($t_s - t_o$) increases toward the event center.

4. Modeling the FTE Ion Data

The general similarity between the observed and modeled ion spectrograms in Figures 5b and 5d suggests that this model can reproduce the observations in considerable detail. This section investigates whether this is the case. *Smith and Owen* [1992] presented the ion distribution function at the center of this event, and a clear cutoff to the D-shaped distribution is observed close to a field parallel velocity of zero. From the theory of *Cowley* [1982] this cutoff would imply that the field line velocity was zero. Such a situation is possible if the effects of the field line "tension" force and of magnetosheath flow are in opposition; the field aligned component of the sheath flow would then be close to the local Alfvén speed, such that the Whalén relation holds for the RD even though the field line is almost stationary in the Earth's frame. Note that any "lateral" boundary tangential motion of the field line (normal to the boundary tangential motion that acts to straighten the field line) would not alter this situation.

This explanation of the lower cutoff velocity of the D-shaped distribution does not mean that the field line velocity has not subsequently increased as the field line accelerates away from the reconnection site. For constant speed of field line motion the low-velocity particles of the D-shaped distribution have the longest flight time and come from the reconnection site. However, if a newly opened field line moves initially slowly and then accelerates, it can catch up with lower-velocity ions injected at the X line (M.P. Freeman, private communication, 1995, see discussion by *Lockwood* [1995]). Ions can therefore have a low velocity, even if the field line is now moving faster. Higher-energy particles will come from further from the X line, where the field line is moving faster and ions are accelerated to higher speeds. In this way the field line acceleration away from the X line raises the field parallel ion temperature. To fit the observed ion density and temperature, yet maintain the D cutoff

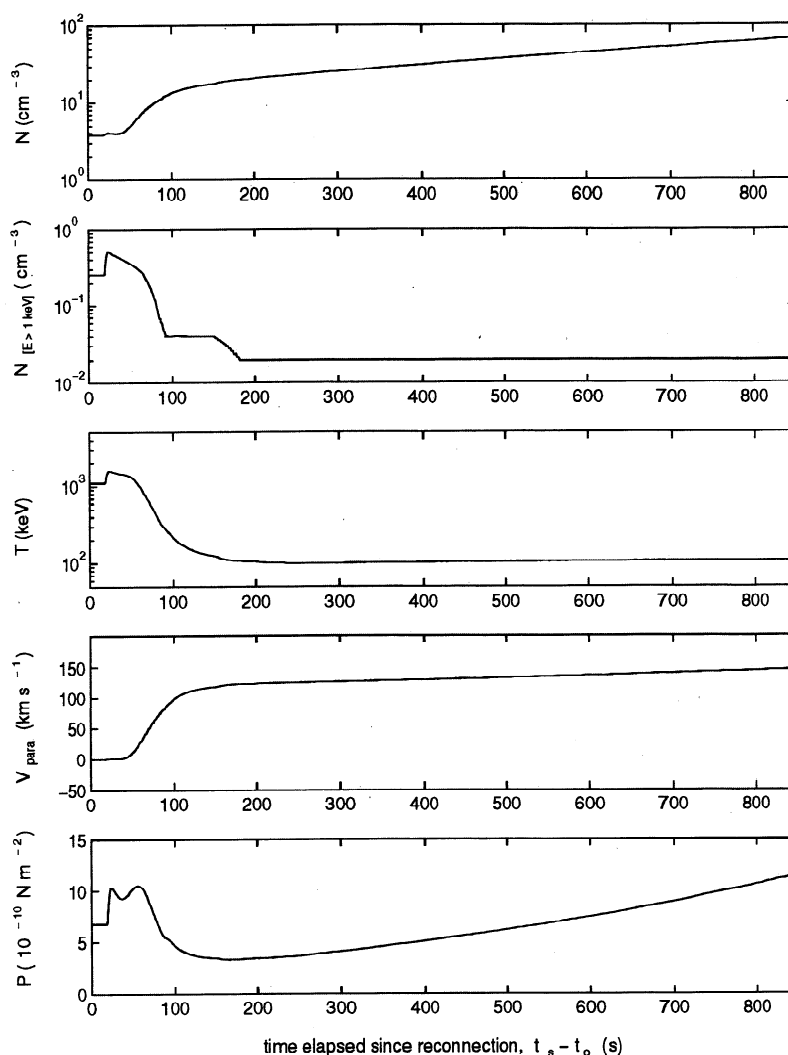


Figure 7. Modeled variations of ion moments as a function of elapsed time since reconnection ($t_s - t_o$) for a satellite $d_a = 8 R_E$ from the X line. From top to bottom: the ion density, N , observed in the instrument energy range of 100 eV–16 keV, the ion density in the energy range 1–16 keV, $N_{[E > 1 \text{ keV}]}$, the ion temperature, T , the field parallel velocity, V_{para} , and the ion pressure, $P = NkT$.

close to zero, we allow the field line to accelerate linearly with time from zero to $V_p = 140 \text{ km s}^{-1}$ at the time of the FTE observation. We assume the reconnection site is $d_a = 8 R_E$ from the satellite (verified in section 7). The ion distribution function in the magnetosheath is taken to be isotropic and of the same temperature as the field perpendicular temperature seen inside the event core by *Smith and Owen* [1992] (i.e., 300 eV). From this distribution function the sheath density is estimated to be 10^8 m^{-3} . The magnetospheric population is as observed by AMPTE UKS outside the event, being at rest with a temperature of 1000 eV and a density of $2 \times 10^6 \text{ m}^{-3}$ and giving an internal Alfvén speed of 800 km s^{-1} . In addition, we adopt reflection and heating factors of magnetospheric ions of 0.6 and 1.3 for the external RD and 0.05 and 1.5 for the internal RD, as inferred by *Lockwood et al.* [1996].

With these inputs we can model the variations of the moments and partial moments of the ion gas with time elapsed since reconnection ($t_s - t_o$), as shown in Figure 7. To compute three-dimensional moments, we simulate the ion distribution functions with allowance for ion flight times (as done by *Lockwood* [1997]), but along field lines of constant field

strength (i.e., mirror forces are neglected). Figure 7 shows (top to bottom) the ion density N , observed in the instrument energy range of 10 eV to 16 keV; the ion density in the energy range 1–16 keV, $N_{[E > 1 \text{ keV}]}$; the ion temperature T ; the field parallel velocity V_{para} ; and the ion pressure $P = NkT$. At $(t_s - t_o) = 0$, i.e., at the magnetic separatrix, the distribution has not yet had time to respond to the reconnection and is as in the magnetosphere, the first sign of change being the arrival of ions at energy $E > 1 \text{ keV}$, which have been reflected off the interior RD. These are seen as a rise in $N_{[E > 1 \text{ keV}]}$ and cause a weak rise in N and T , with a more significant increase in P . These energetic ions decay away because the source magnetospheric population is lost, by transmission through the magnetopause, the drop taking place in two steps because some ions are initially reflected and then lost after mirroring close to the Earth and returning to the magnetopause. Subsequently, $N_{[E > 1 \text{ keV}]}$ is set to a constant noise level. From about $(t_s - t_o) \approx 50 \text{ s}$ onward, sheath ions arrive, causing a rise in N and V_{para} and a fall in T . However, after $(t_s - t_o) \approx 200 \text{ s}$, T begins to rise again slightly because of the field line acceleration away from the X line. This effect, along with the rising N , contributes to a sustained rise in P .

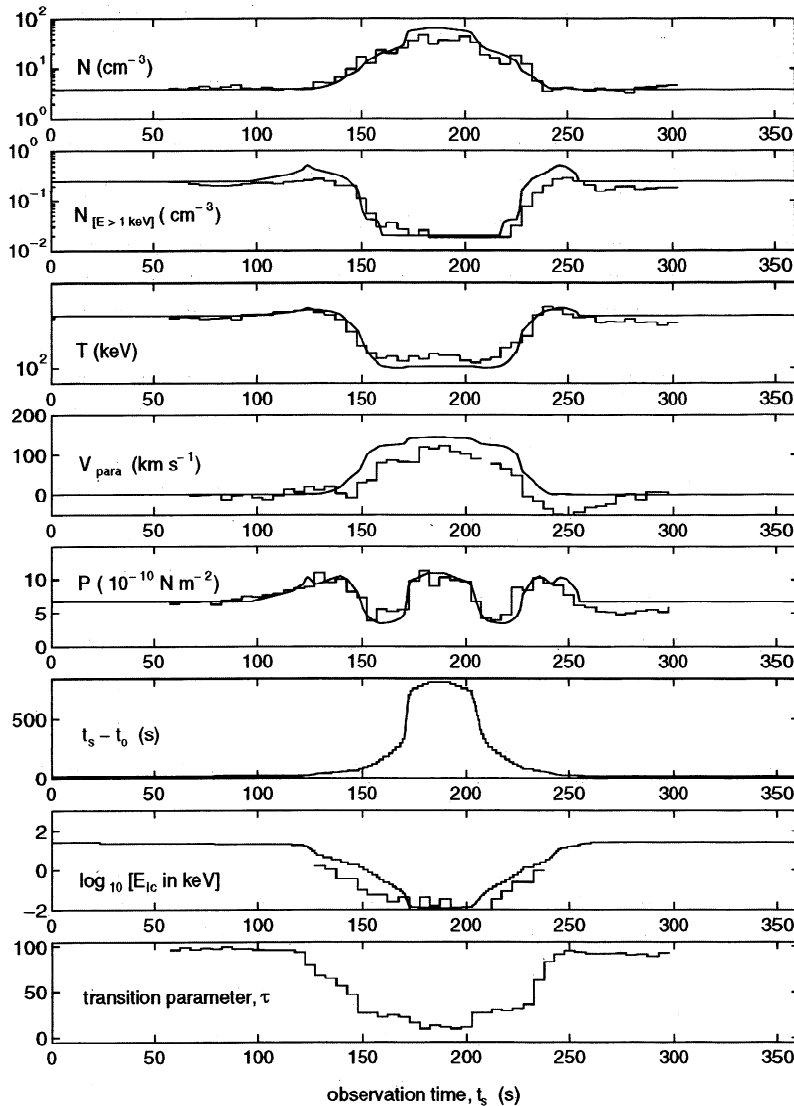


Figure 8. Observed (histograms) and best-fit modelled (curves) moments of the ion gas, as a function of the observation time t_s . (top to bottom) Ion density N , observed in the instrument energy range of 100 eV to 16 keV; ion density $N_{[E > 1 \text{ keV}]}$ in the energy range 1–16 keV; ion temperature T ; field parallel velocity V_{para} ; ion pressure P ; best fit time elapsed since reconnection ($t_s - t_0$); low-energy ion cutoff E_{ic} ; and the observed electron transition parameter τ .

Figure 8 shows the results of fitting these variations to the observed moments shown as a function of t_s (given on the figure axis in seconds after 1043 UT). The histograms are the observed values, and the lines are the fitted model values. The procedure adopted was to vary the value of the time elapsed since reconnection ($t_s - t_0$) at every observation time t_s , until the best fits to N and T were obtained. This prescribes the variation in P , but $N_{[E > 1 \text{ keV}]}$ and V_{para} are independent tests of these fits. Figure 8 also shows the fitted ($t_s - t_0$). As a further test the time-of-flight cutoff energy of the ions, E_{ic} , is computed from the ($t_s - t_0$) and compared with the observed value. The bottom panel of Figure 8 shows the electron transition parameter, which will be discussed in section 5.

Figure 8 clearly shows that the model can explain the variation of the moments of the ion gas within the event. In fact, it provides a first explanation of the ion pressure variation in the event, as reported by *Rijnbeek et al.* [1987] and *Farrugia et al.* [1988]. On the edges of the event, on open field lines between the magnetic separatrix and the interior RD, is a region of

slightly enhanced ion temperature and considerably enhanced pressure. The second panel shows that there is a slight rise in ion number density at the higher energies in this region, and the model explains these enhancements as ions of magnetospheric origin reflected off the interior RD. The spectrogram shown in Figure 5d and Plate 1 of *Farrugia et al.* [1988] shows that these ions are not seen in the center of the event. Therefore they are not of magnetosheath origin, for example, accelerated by the bow shock [*Fuselier, 1998*]. A layer of field lines that have been reconnected longer are then seen inside the interior RD, the particle pressure is low here because magnetospheric ions have been lost, but only the more energetic magnetosheath ions have arrived. Last, at the event core the particle pressure is high because field lines have been open long enough for most of the sheath population to have arrived. In addition, the temperature is slightly higher here than in the outer part of the event because of the acceleration of the reconnected field lines away from the reconnection site. This acceleration will allow the point where the field line threads the magnetopause to catch up with some

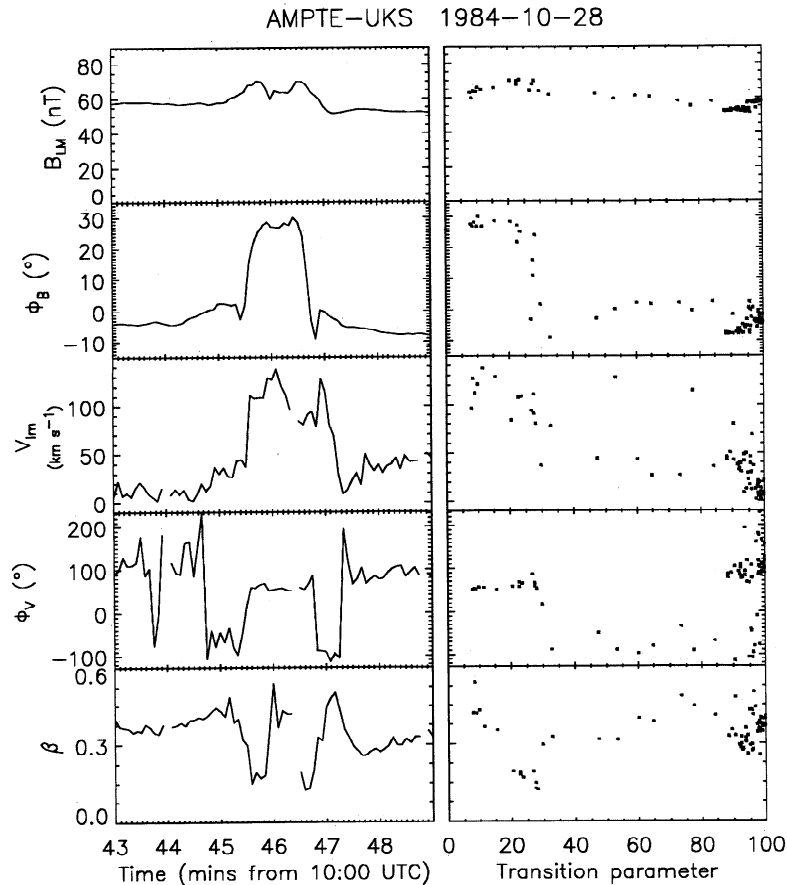


Figure 9. Observed variables as a function of (left) observation time t_s , and (right) transition parameter τ . (top to bottom) Boundary tangential magnetic field, B_{LM} (to the nominal magnetopause); angle that the tangential field makes with the L direction, ϕ_B ; tangential component in the ion flow, V_{LM} ; angle that the tangential flow makes with the L direction, ϕ_V ; and plasma β .

ions injected earlier, and these ions will be either reflected back into the magnetosphere or transmitted through the magnetopause and so returned to the magnetosheath as discussed by Lockwood [1995], based on a suggestion by M.P. Freeman (private communication, 1995). These reflected ions will complicate the injected spectra. Near-zero velocity ions could be observed if the acceleration of the field line were initially slow, allowing the ions to stay ahead of the point where the field line threads the magnetopause. The low-velocity cut off would then be the average speed of the event propagation between the reconnection site and the satellite. In this simulation, with linear acceleration, this average field line speed is 70 km s^{-1} , giving a minimum ion energy of 25 eV.

A significant finding of this modeling is that the field lines at the event center had been open for about $(t_s - t_o) \approx 800 \text{ s}$, yet had moved only $d = 8 R_E$ (in section 7 we present evidence that this is approximately the correct value for d). This very slow evolution of the newly opened field lines can only have arisen from the forces on the reconnected field lines due to sheath flow and tension force being in opposition. We note that the sheath density observed when the satellites emerge through the local magnetopause is $5 \times 10^7 \text{ m}^{-3}$, which is half that inferred from our ion model. This finding indicates that the reconnection site was closer to the subsolar point than were the satellites. The location and evolution of the field lines are discussed further in section 8.2.

5. Event Structure

The magnetopause transition parameter was based on the work of Hall *et al.* [1985] and Bryant and Riggs [1989] and was developed by Hapgood and Bryant [1992]. This parameter exploits the observed anticorrelation of electron density and temperature, also noted by Schopke *et al.* [1981], Phan *et al.* [1997], and Ku and Sibeck [1998]. This can be explained as the change in the moments with a changing ratio of the magnetosheath to the magnetospheric components of an electron gas. Thus, for example, an increased sheath component of the electron gas will decrease the temperature of the total distribution while increasing the density. Almost any process that causes a mixing of the two electron populations (of which reconnection is just one example) could cause this behavior. Thus the existence of a transition parameter is not surprising. What is extraordinary is how well it orders independently measured parameters such as the magnetic field, the ion spectrum and the flow [Hapgood and Bryant, 1992]. From an analysis of the FTE studied in this paper, Lockwood and Hapgood [1997] have shown that this ordering is consistent with the transition parameter being a function of elapsed time since reconnection $(t_s - t_o)$, and they were able to reproduce the electron behavior using the modeling of the ion gas discussed in section 4 with the addition of a potential barrier at the magnetopause, such that the electron behavior maintains quasi-neutrality. As in

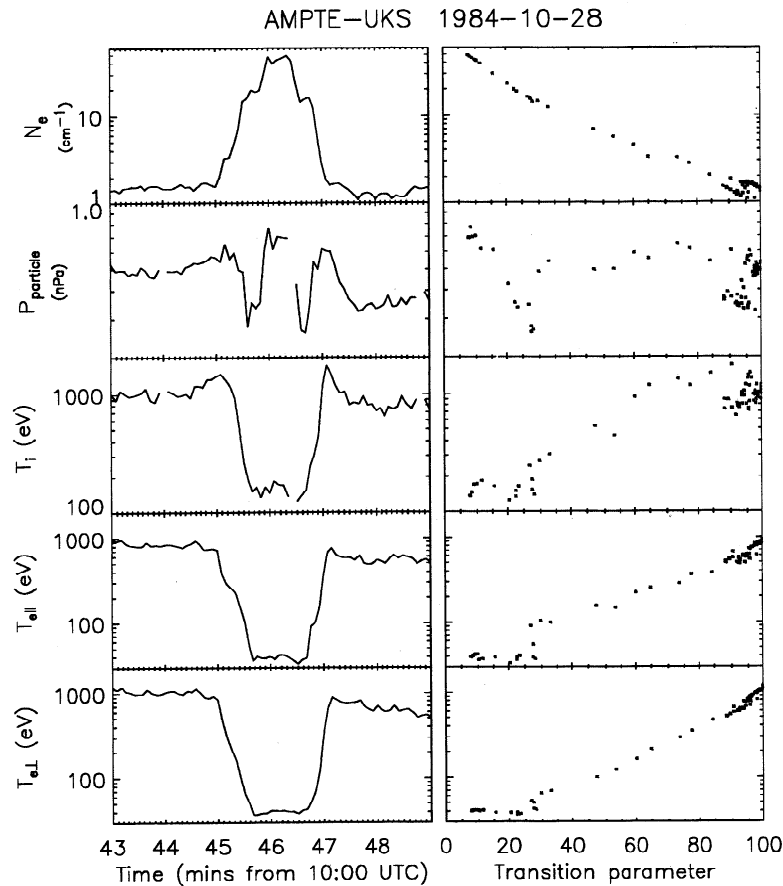


Figure 10. Same as Figure 9 for (top to bottom) electron density N_e ; total particle pressure P ; ion temperature T_i ; parallel electron temperature $T_{e||}$; and perpendicular electron temperature $T_{e\perp}$.

the analysis by Lockwood and Hapgood [1997], the transition parameter τ is here calibrated from the magnetopause crossing at 1145-1245 UT (see their Figure 1). The observed electron density and perpendicular electron temperature are compared with the calibration curve for the magnetopause crossing, and the value of τ is ascribed according to its position along that curve, 0 being at the magnetosheath end of the curve and 100 being at the magnetospheric end. The derived variation of the transition parameter τ in the FTE is shown in the bottom panel of Figure 8.

Figures 9, 10, and 11 study the event structure. Various parameters are plotted, on the left-hand side as a function of observation time and on the right-hand side as a function of transition parameter τ . The panels in Figure 9 show (top to bottom) the boundary tangential magnetic field B_{LM} (to the nominal magnetopause); the angle that the tangential field makes with the L direction, ϕ_B ; the tangential component in the ion flow, V_{LM} ; the angle that the tangential flow makes with the L direction, ϕ_V ; and the plasma β . For Figure 10 they show the electron density N_e ; the total particle pressure P ; the ion temperature T_i ; the parallel electron temperature $T_{e||}$; and the perpendicular electron temperature $T_{e\perp}$. For Figure 11 they show the pressure anisotropy factor $\alpha = (P_{||} - P_{\perp})/\mu_0 B^2$, where $P_{||}$ and P_{\perp} are the total field perpendicular and field parallel particle pressures; the magnetic pressure P_{mag} ; the field parallel component of the ion flow, $V_{||}$; the field parallel component of the electron flow velocity, $V_{e||}$; and the electron anisotropy, $A_e =$

$(T_{e||}/T_{e\perp})/(T_{e||} + T_{e\perp})$. Regions of counterstreaming electron flows are marked by high A_e and coat both edges of the event. At the center of each counterstreaming region the bulk electron flow reverses from away from the Earth ($V_{e||} < 0$) on the outside to toward the Earth ($V_{e||} > 0$) in the event center. The region of earthward ion flow is nested within the earthward electron flow, and the counterstreaming electrons persist in the gap between the two. This behavior strongly implies that the counterstreaming is associated with the maintenance of quasi-neutrality in the region where large electron fluxes can run ahead of the ion fluxes. The value of α is computed from the ion anisotropies given by Smith and Owen [1992] and the electron anisotropy shown in Figure 11. Note that in the event center, the α falls to -0.1 because of the D-shaped ion velocity distributions, making $T_{i||} < T_{i\perp}$. On the edges of the event this ion pressure anisotropy is countered by the electron anisotropy in the region of counterstreaming electrons, where $T_{e||} > T_{e\perp}$, and as a result, α is near zero on the event edges.

Because the event is a relatively straightforward passage into the LLBL, the structure seen on entering and leaving the event in the left-hand plots is not appreciably different from that in the right-hand plots. The right hand plots do stress that most parameters are broadly the same on entering and leaving the event. We here use the transition parameter τ to identify features as a matter of convenience (each feature appearing at two observation times t_s in the left-hand plot but only one τ in the right-hand plots).

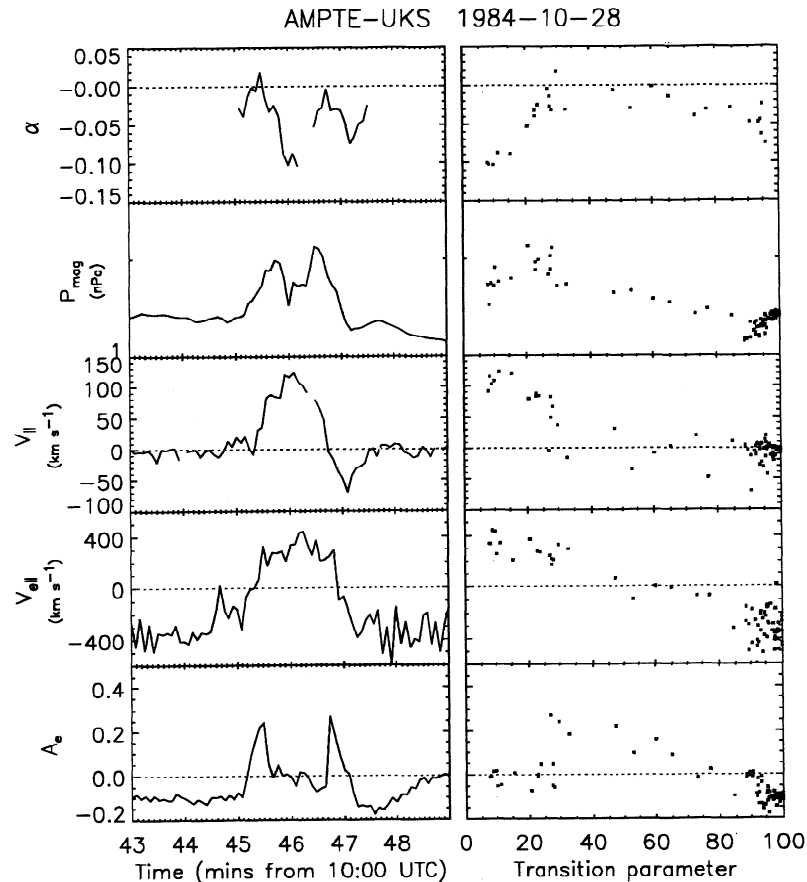


Figure 11. Same as Figure 9 for (top to bottom) pressure anisotropy α (equal to $(P_{||} - P_{\perp}) \mu_0 / B^2$, where $P_{||}$ and P_{\perp} are the field parallel and field perpendicular particle pressures); magnetic pressure P_{mag} ; field parallel ion flow $V_{||}$; field parallel electron flow velocity $V_{e||}$; and electron anisotropy A_e , defined as $(T_{e||} - T_{e\perp}) / (T_{e||} + T_{e\perp})$.

As τ increases from 14 to 28.5, there is a rotation (40°) in the magnetopause tangential field B_{LM} , seen in the angle ϕ_B . Here, densities are roughly halfway between those at the event center and those in the magnetosphere, and the rotation is accompanied by a change in the strength of this field component, a fall in $V_{||}$ to zero, and a rotation in the tangential flow (seen as a 160° change in ϕ_V). On the edge of this rotation ($\tau \approx 28.5-30$) are step-like increases in the particle pressure and the electron and ion temperatures, a sudden onset of counterstreaming electrons, a decrease in the boundary tangential flow, V_{LM} , and some rotation in the boundary tangential field. A steady, but small, field rotation is seen at $\tau \approx 30-60$, and elevated ion temperatures are seen at $\tau > 50$; these are explained in section 4 as magnetospheric ions reflected off the interior RD, which calls for it to be at $\tau < 50$ (i.e., on the magnetosheath side of the elevated ion temperatures). The counterstreaming electron flows, as revealed by $A_e > 0$, are seen at $\tau \approx 30-60$, and the net electron flows are field aligned in the event core but reverse at $\tau \approx 50$, in the middle of the region where the counterstreaming is seen. Accelerated boundary tangential flows are mainly found at $\tau < 30$, but there are four anomalously large points seen on leaving the event. These are the only data points not well ordered by the transition parameter.

The field parallel electron flows at the event center are positive, i.e., in the same direction as the field; this is also true for the field parallel ion flows. This region is dominated by the

high-density, low-temperature sheath plasma flowing into the magnetosphere and also flowing parallel to the magnetic field. This defines the connectivity of the open field lines in the event center, which must map to the northern hemisphere. This connectivity is consistent with the location of the satellite (at GSM latitude $+25.7^\circ$ in the northern hemisphere) and a reconnection site southward of this location.

6. Analysis of the Field Rotation and Flow in the Event

Figure 12 shows the fields and flows seen by AMPTE UKS (thick line) and IRM (thin line). From top to bottom the figure shows the transition parameter τ ; the L, M, and N components of the magnetic field (the coordinate frame being determined from the magnetopause crossing later in the UKS pass), B_L , B_M , and B_N ; the L, M, and N components of the field perpendicular ion flow, $V_{L\perp}$, $V_{M\perp}$, and $V_{N\perp}$; and the field parallel flow $V_{||}$. The event is defined by the characteristic variation in B_N , which is simultaneous in the data from both satellites, to within the 5-s resolution. Changes in B_L and B_M are also simultaneous on the outside of the event (in the weak rotation identified in the previous section) but are nested for the larger rotation on the edges of the event core, in a manner consistent with UKS's position closer to the magnetopause. The flow components also show this nesting at the event center.

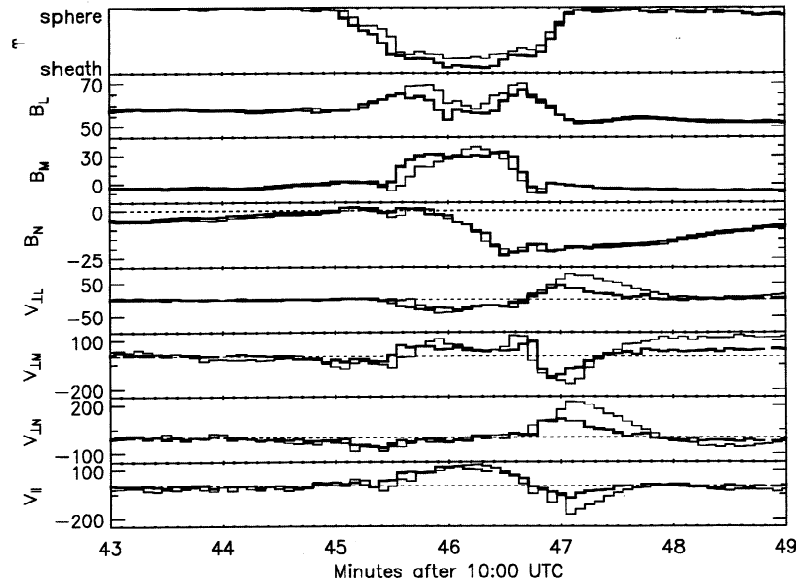


Figure 12. Flows and fields seen by AMPTE UKS (thick line) and IRM (thin line). (top to bottom) Transition parameter τ ; L, M, and N components of the magnetic field B_L , B_M , and B_N and of the field perpendicular ion flow V_{LL} , V_{LM} and V_{LN} ; field parallel flow $V_{||}$. UKS was situated 180 km closer to the magnetopause than was IRM.

Note that the transition parameter seen in the event center by IRM is larger than that seen by UKS. This finding confirms that IRM does not go as deep into the event center as does UKS, because it is 180 km further away from the magnetopause. This also gives us some calibration of the transition parameter in terms of a spatial extent, as we know that $\tau \approx 10$ (seen by UKS at event center) is 180 km closer to the magnetopause than $\tau \approx 20$ (seen by IRM at the event center). This calibration factor will change with τ , but if it is applied linearly to the larger field rotation at $\tau = 14$ –28.5, it gives a boundary normal width of 260 km (see section 8.3).

The anomalous flows seen on leaving the event (particularly at 1046:45–1048:00 UT) are even more marked in the IRM data and are caused in large part by large negative field parallel velocities, i.e. directed from the magnetosphere and toward the boundary. In analyzing the flows around this event, *Sibeck and Smith* [1992] did not differentiate between field parallel and field perpendicular flow. The field perpendicular flows in the regions draped over the event core, as shown in Figure 12, are consistent with an asymmetric passing bulge in the boundary (as predicted by both models in Figure 6), with the boundary being more steeply tilted on the trailing edge of the bulge.

Figure 13 summarizes the orientation of fields and flows at the center of the event and in the surrounding magnetosphere in the local LM, boundary tangential plane; \mathbf{B}_{sp} is the magnetospheric field, and \mathbf{B}_{fe} is the field in the center of the FTE. The flow vector \mathbf{V}_{fp} is the component of the motion of the field lines in the direction of \mathbf{B}_{fe} used as an input to the model to obtain the observed temperature T and pressure P in the event core. The velocity \mathbf{V}_\perp is the observed field perpendicular motion in this LM plane. The vector sum of \mathbf{V}_{fp} and \mathbf{V}_\perp is the field line velocity \mathbf{V}_f , which is appreciably different from the sheath flow velocity \mathbf{V}_{sh} , seen when the satellite emerges into the magnetosheath. The difference can be attributed to the velocity \mathbf{V}_t , caused by the curvature “tension” force on the field lines. The velocity \mathbf{V}_{diff} is discussed below.

We now apply the “tangential stress balance test” to the main rotation in the field seen on the edges of the event core. We use

the test, as prescribed by *Paschmann et al.* [1979, 1986], and plot each component of the ion velocity, V_x , against $(\rho/\rho_0)B_x$, where B_x is the component of the field in the same direction and ρ is the mass density, which has a value of ρ_0 at a reference point in the field rotation. Figure 14 shows the results for the L, M, and N components during the larger (outer) rotation, which is selected by requiring the transition parameter τ to be in the range 14–28.5. Notice that this means that data from two distinct periods, on entering and leaving the event, are used.

An anticorrelation is found in all three cases, the correlation coefficients being -0.53 , -0.33 and -0.59 for the L, M, and N components, respectively, which are significant at the 93%, 81%, and 95% confidence levels. The fitted slopes are -0.8 ± 0.5 , -0.7 ± 0.5 , and $-0.7 \pm 0.5 \text{ km s}^{-1} \text{ nT}^{-1}$. The results of this test are not altered if data from the core of the FTE ($\tau = 0$ –14) are included and significance levels are increased to 99%, 81%, and 98%. However, if data from $\tau > 28.5$ are included (across what we suspect is the interior RD), the correlations are degraded.

In section 5 we established that this event is connected to the northern hemisphere with negative boundary normal field at the magnetopause. Figure 15 shows a simple picture of such an open LLBL with exterior and interior disturbances (here shown as RDs but valid for any Alfvénic disturbance), e and i, propagating into the inflow on the magnetosheath and magnetospheric sides, respectively. The Alfvénic disturbances propagate at a speed $V_A f$, where V_A is the local field aligned Alfvén speed and f is a factor that depends on the type of disturbance [*Heyn et al.*, 1988] (for example, $f = 1$ for an RD; $f > 1$ for a slow mode shock or a slow mode expansion fan; and $f = \infty$ for a contact discontinuity). The vector addition of the field line velocity, \mathbf{V}_f , and the inflow into the reconnection layer, \mathbf{V} , gives field aligned flow speed of $V_A f$. This field aligned flow is parallel to the field for the exterior discontinuity but antiparallel for the interior one for this case with $B_n < 0$. This gives

$$\mathbf{V} = \mathbf{V}_f \pm (\mathbf{V}_A / f) = \mathbf{V}_f \pm (\mathbf{B} / f) \{ (1 - \alpha) / \mu_0 \rho \}^{1/2} \quad (1)$$

where the plus and minus signs, in this case with $B_n < 0$, relate to the e and i disturbances, for which the field parallel flow in

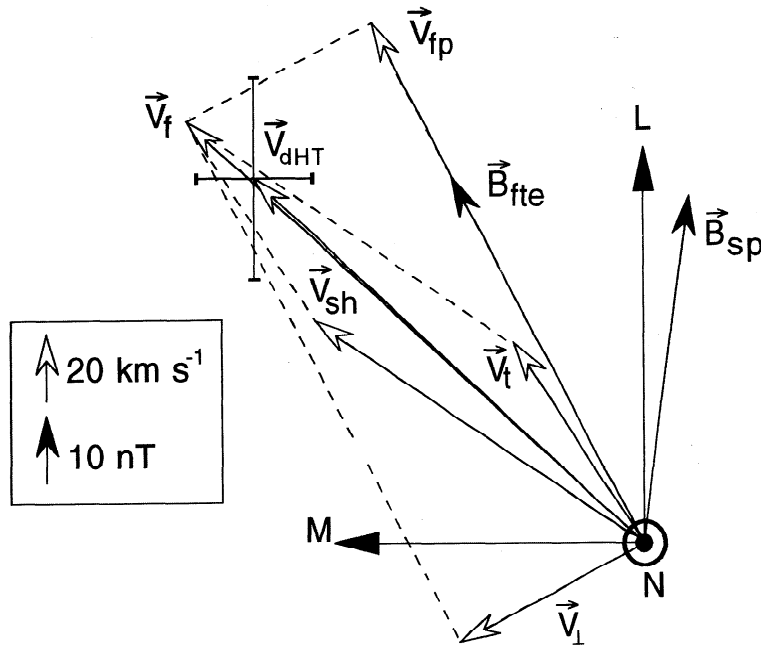


Figure 13. Vector representation of the fields and flows in and around the FTE event: magnetospheric field \mathbf{B}_{sp} ; field in the center of the FTE \mathbf{B}_{fte} ; component of the motion of the field lines in the direction of \mathbf{B}_{fte} , \mathbf{V}_{fp} (used in the fits in Figure 8); field perpendicular velocity in the LM plane, \mathbf{V}_f ; field line velocity \mathbf{V}_f ; sheath flow velocity \mathbf{V}_{sh} ; velocity caused by the curvature “tension” force on the field lines, \mathbf{V}_t ; de Hoffman-Teller frame velocity \mathbf{V}_{dHT} (derived from the stress balance test shown in Figure 14).

the field line rest frame (the “de Hoffman-Teller frame” [de Hoffman and Teller, 1950], V_{fj} , is positive and negative, respectively. Equation (1), being a linear vector equation, is valid for any component. This equation is a generalized version of that used to test for an RD ($f = 1$) in the tangential stress balance test [Paschmann *et al.*, 1979; Sonnerup *et al.*, 1981, 1986]. Putting into a form equivalent to that used by Paschmann *et al.* [1979], but without actually applying the mass conservation condition for an RD (derived by Hudson [1970]), we get

$$\mathbf{V} = \mathbf{V}_f \pm (\rho_o/\rho)\mathbf{B} (1/f) \{ (1-\alpha)\rho/\mu_o\rho_o^2 \}^{1/2} \quad (2)$$

Thus the negative slopes in Figure 14 show that this field rotation is an interior disturbance (i) and is not an exterior one (e), because $B_N < 0$. The field parallel component of the de Hoffman-Teller velocity is $+140 \text{ km s}^{-1}$ (where velocities are defined as positive parallel to \mathbf{B}) and thus transforming the field parallel velocity in the Earth’s frame V_{fj} (of magnitude less than 30 km s^{-1} , as shown in Figure 11) into the de Hoffman-Teller frame gives $V_{fj} < 0$ (i.e., flow antiparallel to \mathbf{B}). This identification of the field rotation as an interior disturbance (i) further reinforces the conclusion of Smith and Owen [1992] and Lockwood and Hapgood [1997] that the satellite did not enter the magnetosheath through an exterior RD (e) in this event.

Equation (2) shows that the slope of the fits for the three components should be the same. In Figure 14 they are -0.8 ± 0.5 , -0.7 ± 0.5 , and $-0.7 \pm 0.5 \text{ km s}^{-1} \text{ nT}^{-1}$. These values are all consistent with a (negative) slope of magnitude $-0.75 \pm 0.50 \text{ km s}^{-1} \text{ nT}^{-1}$. The reference point used is at $\tau = 15$, for which the number density is $N_o = 3 \times 10^7 \text{ m}^{-3}$ (Figure 10), the field strength is $B_o = 65 \text{ nT}$ (Figure 9), and $\alpha_o = -0.09$. The main unknown in (2), apart from f , is the mean ion mass (ρ_o/N_o). We

here use three assumptions for the composition of the ion gas: (1) pure protons, giving a mean ion mass of 1 amu; (2) 5% He^{++} or He^+ with 95% protons, giving a mean ion mass of 1.15 amu; and (3) 5% He^{++} or He^+ , 93% protons and 2% ionospheric O^+ , giving a mean ion mass of 1.45 amu.

Figure 14 indicates that there is an Alfvénic discontinuity of some kind (see review by Lin and Lee [1993a]), either an RD (also called an intermediate mode, or Alfvén wave), a slow mode shock or a slow mode expansion fan. If we consider an RD, $f = 1$ and the Hudson [1970] mass conservation condition applies, i.e., $(1-\alpha)\rho$ is constant. The theoretical slope from equation (2) is thus $\{ (1-\alpha_o)/\mu_o\rho_o \}^{1/2}$ and using the observed N_o and α_o yields slope magnitudes of (1) 4.2, (2) 3.9 and (3) 3.5 $\text{km s}^{-1} \text{ nT}^{-1}$ for the three composition cases (1), (2) and (3) above. Therefore this is not a successful application of the Whalén relation (for an RD) because the observed slope of magnitude $0.75 \pm 0.50 \text{ km s}^{-1} \text{ nT}^{-1}$ is inconsistent with $f = 1$ for any reasonable ion composition assumption. Nor is the structure a contact discontinuity for which $f = \infty$; equation (2) predicts that this value would give a slope of zero (for any composition of the ion gas), which is also outside the observed range of $0.75 \pm 0.50 \text{ km s}^{-1} \text{ nT}^{-1}$.

Next we investigate whether the putative Alfvénic discontinuity could be a slow shock or a slow mode expansion fan. Heyn *et al.* [1988] show that $\eta < 1$ for the former but $\eta > 1$ for the latter, where

$$\eta = (B_{t2}/B_{t1}) = \{ 1 + \beta(1 - P_2/P_1) \}^{1/2} \quad (3)$$

where B_t is the discontinuity tangential magnetic field and P is the particle pressure and the subscripts 1 and 2 refer to upstream and downstream of the discontinuity. From the sense of the slope in Figure 14 and because the field parallel flow is negative

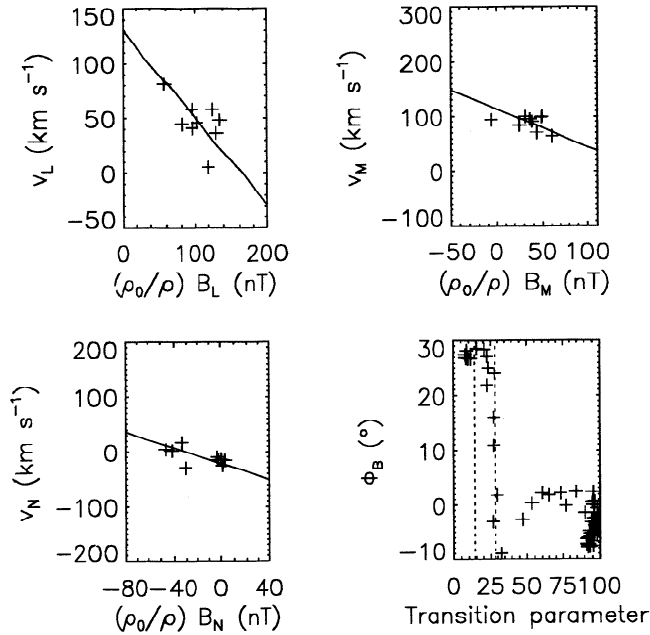


Figure 14. Stress balance tests applied to the major field rotation on the edges of the FTE core. Regression plots of velocity component V_x and magnetic field component, B_x , for x of (a) the L, (b) the M, and (c) the N directions, and (d) the angle that the tangential field makes with the L direction, ϕ_B , as a function of the transition parameter, τ . The vertical lines in Figure 14d show the transition parameter range 14–28.5 used to select the data in Figures 14a, 14b, and 14c.

in the de Hoffman-Teller frame, we know that the upstream side is the magnetospheric side of this structure. Figure 10 shows that P increases steadily in the downstream direction (i.e., decreasing τ) through this structure, so $P_2 > P_1$ and thus by (3), $\eta < 1$. Therefore this structure is most likely to be a slow shock rather than a slow expansion fan. The plasma $\beta = 2P\mu_0/B^2 \approx 0.15$, and from the values of N , T_e , and T_i shown in Figure 9 upstream and downstream of the discontinuity, equation (3) yields $\eta \approx 0.92$. However, a shock is surprising, considering the extended nature of the density change (estimated above to be of the order of 250 km) [see Lin and Lee, 1993a].

The equations of Heyn *et al.* [1988] assume pressure isotropy ($\alpha = 0$), which Figure 11 shows is a good approximation on the edges of the event. From them we can derive an expression for the factor f appropriate to a slow shock:

$$f = (\rho_1/\rho_2)^{1/2} \{1 + (1+\eta)/[\gamma\beta + (\gamma-1)(1-\eta)]\}^{1/2} \quad (4)$$

where γ is the polytropic index. Pudovkin *et al.* [1997] use theory and past observations to estimate that γ is between 1.34 and 1.95 at the bow shock, but pressure anisotropy at the magnetopause means that the effective γ can be less than 1. We here use the adiabatic law,

$$\rho_1/\rho_2 = (P_2/P_1)^{1/\gamma} \quad (5)$$

for the ratios of the densities and pressures across the structure to estimate $\gamma = 1.2$. Using this and the mean $\beta = 0.15$ (see Figure 9), we find that equation (4) yields $f = 2.7$ for a slow shock. Using the mean N and α of $2 \times 10^7 \text{ m}^{-3}$ and -0.05 ,

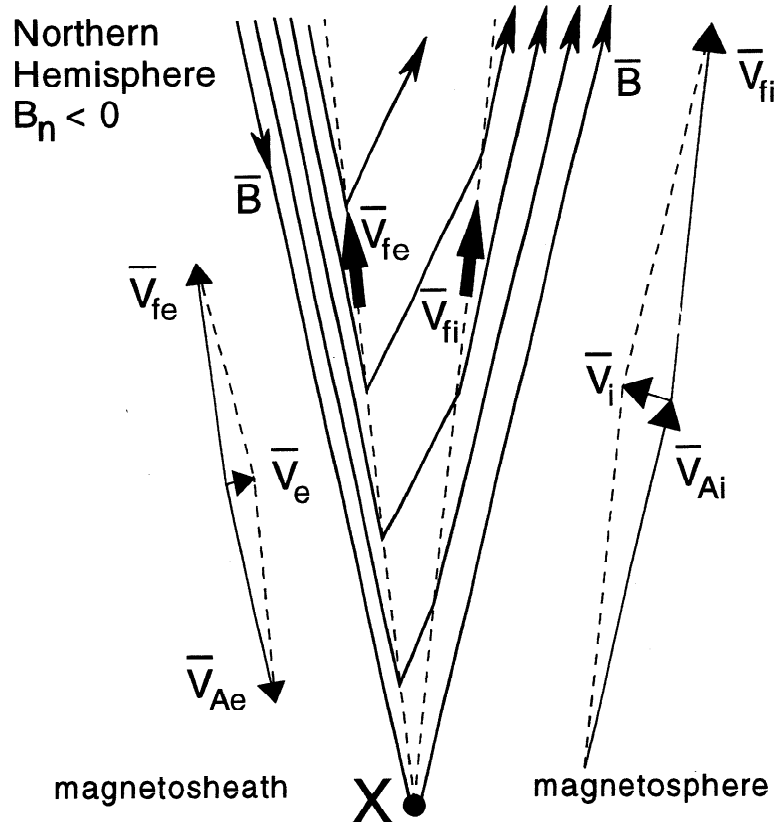


Figure 15. Schematic illustration of two Alfvén waves (RDs) propagating away from the reconnection site X into the magnetosheath and magnetospheric inflow regions where the Alfvén speed is V_{Ae} and V_{Ai} , respectively, and $B_N < 0$. The exterior and interior disturbances (dashed lines) move at V_{fe} and V_{fi} and the inflow toward the boundary is V_e and V_i in the Earth's frame, giving the vector sums $V_{fe} + V_{Ae} = V_e$, as illustrated in the left-hand vector addition and $V_{fi} - V_{Ai} = V_i$, as illustrated in the right-hand vector addition.

respectively, we find from equation (2) theoretical slopes of (1) 1.2, (2) 1.1, and (3) 1.0 $\text{km s}^{-1} \text{nT}^{-1}$ for the three composition assumptions. These values are still somewhat higher than the nominal observed value, but all are consistent with it to within the uncertainty. Hidden mass (ions at energies either above or below the 10 eV to 16 keV range of the instrument and/or higher percentages of heavier mass) would mean that the above values should be reduced. Thus a slow mode shock is a possibility. We also note that the values computed for f depend sensitively on α in this case because η is so close to 1.

For completeness, from the equations given by Heyn *et al.* [1988] we can also derive an expression for f for a slowmode expansion fan,

$$f = (1 + V_{at}^2 / C_s^2) = \{1 + B_i^2 / (\gamma P \mu_0)\}^{1/2} \quad (6)$$

where V_{at} is the boundary tangential Alfvén speed (corresponding to B_i) and C_s is the sound speed equal to $(\gamma P / \rho)^{1/2}$. This gives $f = 3.5$ for a slow mode expansion fan and theoretical slopes for the stress balance test of (1) 1.0, (2) 0.9, and (3) 0.8 for the three composition assumptions. These are all within the range of possible experimental values for the magnitude of the slope of $0.75 \pm 0.50 \text{ km s}^{-1} \text{nT}^{-1}$ and similar to those for the slow shock.

From the above we find that the field rotation on the edges of the FTE core is a convecting structure and the consistency of the slope in the three components suggests it may be an Alfvénic discontinuity, but its speed of propagation is lower than that of an Alfvén wave (RD) and is most likely to be a slow shock. On the magnetospheric side of this structure, $V_{\parallel} < 0$ (i.e., flow antiparallel to \mathbf{B}) in the Earth's frame, as the flow is dominated by the escape of magnetospheric ions toward the magnetopause: nearer the magnetopause, within and on the other side of this structure, $V_{\parallel} > 0$ as the flow is dominated by injected magnetosheath ions flowing earthward.

From the intercept of any component of \mathbf{B} , $B_x = 0$ in Figure 14, equation (2) shows we can derive the corresponding component, V_{fx} , of the de Hoffman-Teller reference frame of the convecting structure. This derivation gives $V_{fx} = 130 \pm 57 \text{ km s}^{-1}$, $V_{fy} = 113 \pm 21 \text{ km s}^{-1}$, and $V_{fz} = -22 \pm 12 \text{ km s}^{-1}$. This motion is plotted in the nominal LM plane in Figure 13 and labeled \mathbf{V}_{dHT} . The experimental uncertainties in this vector are also shown. To within these uncertainties, \mathbf{V}_{dHT} is the same as the \mathbf{V}_f deduced from the measured values of \mathbf{V}_\perp and the \mathbf{V}_p inferred in section 4. Thus the two separate analyses, given in this section and in section 4, yield a consistent view of a moving structure in the open LLBL.

Last, we also tried to apply the stress test to the discontinuities in the observed temperatures (at $\tau = 28\text{--}30$) in an attempt to define them as being at the internal RD. However, the small field rotation and the very low number of data points in this region do not allow any significant test to be made. Moving toward the magnetosphere, this structure is marked by the onset of a strong electron anisotropy, the cessation of the accelerated flow region, a drop in magnetic pressure, and a rise in particle pressure. The mass conservation condition that $\rho(1-\alpha)$ is constant applies across this feature, and the rise in particle pressure is comparable with (but slightly smaller than) the loss in magnetic pressure. The local Alfvén speed is about 650 km s^{-1} , slightly lower than, but not inconsistent with, the 750 km s^{-1} employed in section 4 to model the ions thought to be reflected off this RD. This Alfvén speed is significantly lower than the value of 1000 km s^{-1} , which applies in the magnetosphere outside the event, because some higher-energy sheath ions have

reached the location of the putative interior RD. Thus if this is indeed the interior RD, this example displays the phenomenon suggested by Lockwood *et al.* [1996], namely, that the interior RD may be progressively slowed by the action of super-Alfvénic injected sheath ions.

On the magnetospheric side of the putative inner RD is a slow field rotation (at τ of 30 to 60 in Figure 9), which we interpret in terms of draping of the field lines over the event core. Application of the stress balance test gives no consistent correlations for this rotation.

7. Which Model Best Explains the FTE?

The success of the ion entry and dispersion model in section 4 strongly supports either the 2-D reconnection pulse model or the pressure pulse model, as they can give the continuous variation of elapsed time since reconnection ($t_s - t_o$) with the observation time t_s , which is required to explain the boundary layer structure of the event. In the pressure pulse model the FTE would be a convecting structure, as indeed it was found to be in the previous section. That structure would move with the region of high pressure in the magnetosheath that is giving the indentation. Figure 13 shows that the structure's motion in the boundary tangential plane, \mathbf{V}_{dHT} , is appreciably different from the sheath flow, \mathbf{V}_{sh} , seen later in the pass. They are not the same to within experimental uncertainties, although one must note that \mathbf{V}_{sh} may have changed in the period of 80 min between the time of the FTE observation and the time when the satellite emerges into the sheath through the magnetopause. The fact that this delay is so large implies in itself a change in the solar wind which resulted in the magnetopause moving outward. The solar wind pressure was monitored by IMP 8 on the dawn flank of the magnetosphere, but there was a data gap starting shortly before the event, and there is no evidence for such decrease. However, the total pressure seen inside the magnetosphere by AMPTE UKS and IRM did decay.

Stronger evidence in favor of the reconnection pulse model comes from estimating the reconnection rate as a function of time. This is done by using an adapted version of the method introduced by Lockwood and Smith [1992], improved by Lockwood [1995] and tested by Lockwood and Davis [1996a]. The reason that the method needs to be adapted is that it was developed for the ionosphere, where the magnetic field strength B can be assumed to be constant. This is certainly not applicable to the magnetopause data presented here. However, we can estimate the amount of magnetic flux moving over unit length at the spacecraft location in each 5-s period to be $\Delta F = \Delta t_s B V_\perp$, where V_\perp is the magnitude of the field perpendicular velocity and $\Delta t_s = 5 \text{ s}$. The product $B V_\perp$ is plotted in Figure 16a as a function of t_s (given on the axis in seconds after 1043 UT). Figure 16b gives the values of the time elapsed since reconnection ($t_s - t_o$), as used to give the fits to the ion data shown in Figure 8 (based on a distance of $d = 8 R_E$ between the satellite and the X line). These values have been interpolated between successive fitted values, to give the time elapsed since reconnection, which applies at the beginning and end of each 5-s period. Thus we know the difference in the reconnection times Δt_o of the field lines detected at the start and end of each 5-s interval. We also know the amount of magnetic flux between those two field lines, and thus we can estimate the reconnection rate $E_t = \Delta F / \Delta t_o$. This estimation assumes that unit length of the reconnection X line maps to unit length at the satellite. The variation of E_t with observation time t_s is shown in Figure 16c. This shows that the

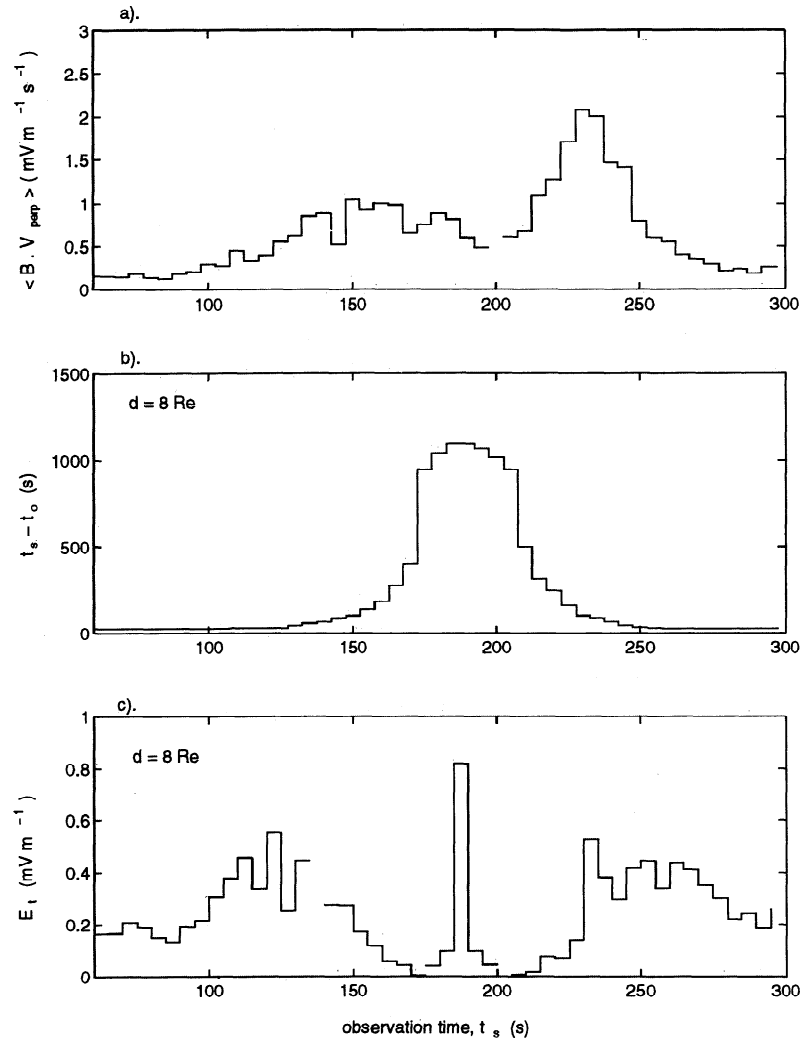


Figure 16. (a) Magnetic flux transported over AMPTE UKS, BV_{\perp} , where V_{\perp} is the magnitude of the field perpendicular velocity and B is the magnetic field strength, as a function of observation time t_s (in seconds after 1043 UT). (b) Time elapsed since reconnection ($t_s - t_o$), for a distance between the X line and the satellite of $d = 8 R_E$. (c) Reconnection rate $E_t = \Delta t_s BV_{\perp} / \Delta t_o$, where $\Delta t_s = 5$ s.

field lines seen at the very center of the event were reconnected at a faster rate than those seen in the outer regions of the event core and in the event boundary layer. Field lines seen on the very outside of the event, on both entry and departure, were reconnected at a high rate.

Figure 17 shows the reconnection rate E_t as a function of the reconnection time t_o (here also given in seconds after 1043 UT). The uncertainties are estimated in the manner described by Lockwood and Davis [1996a]. The plot shows a reconnection pulse at about 50–300 s (roughly 1044–1048 UT) with a long period of slow (almost zero) reconnection at -800 to $+50$ s (i.e., about 1030–1044 UT), before which is seen the end of a prior pulse. It has been assumed that neither the reconnection site (and hence d) nor the locus of evolution of the newly opened flux changes with time. The choice of the distance d is crucial. For other values the points seen on the way into the event do not agree with those seen on the way out, and d has been iterated to the value of $8 R_E$ (with an uncertainty of about $\pm 1 R_E$) employed here to give a coherent variation with t_o . Figure 17 shows that the reconnection is pulsed in rate, as required by the reconnection pulse model. However, the situation is not as simple as Figure 6a implies.

At the center of the event we see field lines reconnected in the first of the two pulses detected in Figure 17. More of this pulse is not seen, because the satellite location in relation to the magnetopause means that it does not get any closer to the event center. The fact that we see the trailing edge of a reconnection rate pulse does not prove in itself that this is what caused the LLBL bulge and thus the FTE event. For the reconnection rate model the existence of such a pulse is necessary, but it is not sufficient as a proof (in the same way that observing a simultaneous pressure pulse in the magnetosheath would be necessary but not sufficient as proof for the pressure pulse model). The outer boundary layers of the event are reconnected in the subsequent pulse, and these more recently opened field lines are draped over the passing bulge caused by the former pulse. Thus the subsequent reconnection history influences the boundary layer structure of the event. Were it not for the inferred outward expansion of the magnetopause after the event, we should have seen this as a second FTE roughly 15 min later, around 1100 UT. Because a subsequent FTE signature was seen by neither of the spacecraft, we infer that the boundary moved out by the order of $1 R_E$ (a typical FTE boundary normal dimension) in the 15 min interval, giving an unremarkable mean

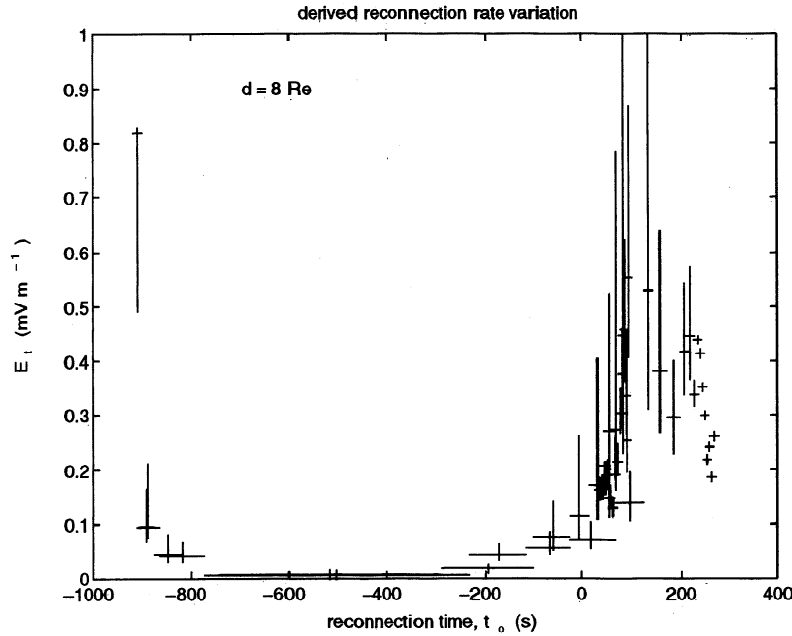


Figure 17. Reconnection rate E_t in Figure 15 shown as a function of reconnection time, t_o , for a distance between the X line and the satellite $d = 8 R_E$.

boundary speed of 7 km s^{-1} . The total pressure falls from $P = 1.8 \text{ nPa}$ just before the FTE to 1.3 nPa at 1100. If we assume pressure balance, such that magnetopause radius is proportional to $P^{-1/6}$, this would correspond to an outward motion of $0.6 R_E$. In section 8.3 we infer that the region of field draping for the FTE extended roughly $0.4 R_E$ earthward of the satellite; thus the inferred outward motion is sufficient for us to fail to see the subsequent event, assuming it to have been of the same size. The role of pressure changes on the detection of FTEs was discussed by *Potemra et al.* [1992]. The inferred outward motion of the boundary is also consistent with the long (80 min) delay between observation of the FTE and the magnetopause.

8. Discussion

We have revealed several features of this magnetospheric FTE event that have not been found by previous studies. The event core has been shown to be a convecting structure, and if this core is bounded by any of the Alfvénic disturbances, it is a slow shock standing in the inflow from the magnetospheric side of the boundary. There is also some evidence for a weak interior RD. The field lines in the core of the event have been shown to have been reconnected in a pulse, and those in the outer layer of the event have been shown to be reconnected in a subsequent pulse. In this way the reconnection rate history explains the layered structure of the event. A model of ion mixing along newly opened field lines explains the pressure structure of the event and shows that the field line had not moved far, despite having being opened for a considerable period of time. We here discuss some further implications of these findings for the structure, motion, and size of the event.

8.1. Event Structure

A de Hoffman-Teller velocity of $V_{dHT} = 170 \text{ km s}^{-1}$ in the tangential plane has been derived for the field rotation on the edge of the core. This rotation forms a “nested” signature in the data from the two craft, being seen by UKS and then IRM on

entry but by IRM and then UKS on exit. The lag is $\Delta t_s \approx 10 \text{ s}$ on the entry into the event, which makes the angle of the bulge with respect to the LM plane of $\omega_{in} = \tan^{-1}(\Delta N / V_{dHT} \Delta t_s) \approx 7^\circ$ (the boundary normal separation of the two craft is $\Delta N = 180 \text{ km}$). On exit from the event the lag was $\Delta t_s \approx 5 \text{ s}$, making this tilt angle larger ($\omega_{out} \approx 13^\circ$). By comparing the values of the B_N component seen, on entry into the event, outside and in the edge of the core we find $\Delta B_N = 7 \text{ nT}$, where the component of B_{LM} in the direction of V_{dHT} is 59 nT (see Figure 11). This yields $\omega_{in} = \tan^{-1}(7/59) \approx 7^\circ$, in agreement with the previous calculation. On the exit from the event, $\Delta B_N = 13 \text{ nT}$, giving $\omega_{out} = \tan^{-1}(13/59) \approx 12^\circ$. Thus the magnitudes of the boundary normal deflections in the bipolar B_N signature are consistent with field lines draped over this asymmetrically shaped bulge of the event core.

It is valuable to compare the structure of the open LLBL seen in this event with that found in a variety of steady state models. *Petschek* [1964] considered the symmetric case (identical plasma in the two inflow regions) and predicted slow shocks standing in the inflow regions on both sides. *Levy et al.* [1964] considered the asymmetric case with the field in one inflow region much larger than that on the other side. The outer slow shock (on the weaker field, i.e., magnetosheath, side) in the Petschek model was replaced by an RD where most of the field rotation occurs and which generates an accelerated flow layer inside the magnetopause. The inner shock was replaced by a slow mode expansion fan where the plasma characteristics evolve from the accelerated flow layer to the magnetosphere proper. More complex simulations and computations predict further structure. *Lin and Lee* [1993a] have reviewed predictions of analytic ideal MHD theory, resistive MHD simulations, and hybrid simulations. The most relevant examples they give are for asymmetric Alfvén speeds across the current layer with a boundary tangential magnetic field in the direction of the X line, shown in their Figures 2.9, Figures 3.8/3.9, and Figures 4.6/4.7, respectively.

From the observations we here infer a possible interior RD from (1) the reflected ions, which appear at high energies on the

edges of the event; (2) the sudden onset of counterstreaming electrons, suggesting the presence of a discontinuity that can also reflect electrons; and (3) the sudden changes in the particle temperatures and pressures. On the magnetosheath side of this the FTE core has here been shown to be a convecting structure that may be an Alfvénic discontinuity; this being the case, a slow shock is the most likely.

For the ideal MHD solutions [Lin and Lee, 1993a, Figure 2.9] an interior RD and a slow mode expansion fan (labeled SE in their plot) are predicted. However, between these a major density drop has sometimes been predicted at a contact discontinuity (CD), and a weak one has been predicted at a slow, interior shock. However, it is not clear why a CD would be present in a collision-free plasma, and it is not seen in the data shown in Figures 9, 10, and 11, which suggest a density decrease more gradual than that predicted at a CD. The predicted slow mode expansion fan is standing in the inflow in the magnetosheath side of the boundary (stress-balance test would give positive slope because $B_N < 0$), whereas the predicted slow shock is standing in the inflow from the magnetospheric boundary, as observed here (stress balance test giving negative slope because $B_N < 0$). This prediction therefore supports our identification of a slow mode shock in preference to a slow mode expansion fan. However, Heyn *et al.* [1988] note that a configuration with an interior slow expansion fan (standing in the magnetospheric inflow) is also possible under certain conditions. The resistive MHD simulations (shown in Figures 3.8 and 3.9 of Lin and Lee [1993a]) also show the contact discontinuity. The main difference is that the interior RD has steepened into a time-dependent intermediate shock (TDIS) in this simulation. Like the ideal MHD calculations they predict that the interior slow mode disturbance is a shock and not an expansion fan. However, the closest model to the observations presented here is undoubtedly the hybrid simulation (shown in Figures 4.6 and 4.7 of Lin and Lee [1993a]). In these predictions the contact discontinuity is absent, and the density gradually decays and the ion temperature increases across the LLBL, as is observed in Figure 10. The field does rotate slightly across this region, but Lin and Lee do not identify this rotation as a slow mode expansion fan. This region marks a transition in the dominant flow (with elapsed time since reconnection) from escaping magnetospheric ions to injected magnetosheath ions flowing earthward. The interior RD is present in the simulations and is seen to reflect ions, as invoked here and by Lockwood *et al.* [1996] (Y. Lin, private communication, 1997). Figure 4.5 of Lin and Lee [1993a] also shows that the hybrid simulation reproduces the D-shaped ion distribution functions in the LLBL, as predicted by Cowley [1982] and observed in the center of this event [Smith and Owen, 1992]. In the simulations the interior RD is marked by small fluctuations in the field, not inconsistent with those seen here at $\tau = 28.5$ –30.

The ion model in section 4 simply allows for ion flight times and the effect of two RDs with no slow shocks or expansion fans. The success of the model in reproducing the observations suggests that the convecting structure at the event core need not be bounded by a slow shock.

The above simulations and calculations are steady state, and some differences are to be expected, as the event is time dependent. Time dependent Petschek reconnection calculations show bulges produced by the reconnection pulse [Biernat *et al.*, 1987; Semenov *et al.*, 1991, 1992a, b; Rijnbeek *et al.*, 1991]. Time dependent MHD simulations can also show these bulges [Scholer, 1988a, b, 1989]. The asymmetric case was considered by Scholer [1989], who also looked at the implications for the

Whalén test (equation (2) for an RD, i.e., $f = 1$). He found that the Whalén relation did not hold in the central bulge, as found here in the FTE. However, there has been some debate as to whether reconnection pulses can produce magnetospheric FTEs at all. Scholer [1989] and Ku and Sibeck [1997, 1998] point out that in the two-dimensional MHD simulations the magnetospheric FTE signatures become so shallow that they vanish for (B_{sh}/B_{sp}) less than about 0.5. This behavior is also found in analytic MHD calculations, but only in the two-dimensional case: in three dimensions with skewed reconnecting fields the analytic calculations do still reveal clear magnetospheric FTEs [Semenov *et al.*, 1992b; V. Semenov, private communication, 1998]. From this finding we would expect to see magnetospheric FTEs, except when B_{sh} and B_{sp} are close to antiparallel and (B_{sh}/B_{sp}) is less than about 0.5. However, we also note that the depth of the indentation of the inner edge of the LLBL in this event is inferred in section 8.3 and found to be rather shallow.

8.2. Event Evolution

The FTE is observed at 9 MLT and at a latitude of 25° , i.e., roughly $4 R_E$ north of the magnetic equator and about $9 R_E$ from the subsolar point, as inferred from pressure balance. From Figure 17 we infer that the satellite was $8 R_E$ away from the reconnection site and that the center of the event was reconnected at 1028 UT, whereas it passed over the satellite at 1046 UT, i.e., 18 min later. Thus the mean speed of the event is just 47 km s^{-1} . For a field line linearly accelerated from rest this would make the low-velocity cut off of the ions 47 km s^{-1} , corresponding to an energy of 10 eV for protons. This happens to be the lower limit of the ion detector, and we would see the cut off as being at zero velocity. Thus the long elapsed time since reconnection, derived from fitting the moments of the ion gas, is consistent with the near-zero cutoff velocity of the distribution function seen at the event center [Smith and Owen, 1992].

The average speed of event motion of 47 km s^{-1} should be compared with the derived components of the boundary tangential velocity of the event at the satellite, which are found from the stress balance test to be $V_{\perp L} = 130 \pm 57 \text{ km s}^{-1}$, $V_{\perp M} = 113 \pm 21 \text{ km s}^{-1}$ (giving a boundary tangential speed of 172 km s^{-1} , close to the value of 160 km s^{-1} inferred from modeling the ion moments). This finding confirms that the flux tube had indeed accelerated.

From the similarity of the inferred distances from the satellite to the reconnection site and to the subsolar point it is possible that the part of the FTE dragged over the satellites was reconnected within about $1 R_E$ of the subsolar point. However, this would mean that the subsequent pattern of motion of the event was somewhat unlikely, having moved about $9.5 R_E$ in the M direction but only about $4 R_E$ in the L direction, yet having accelerated to a faster speed in the L direction. Thus it seems likely that the part of the event that moved over the satellites was reconnected between 9 and 12 MLT and in the southern hemisphere. The sheath density of 10^8 m^{-3} required to fit the ion data is roughly twice that seen when the satellites finally emerge into the sheath. This increase implies a reconnection location closer to the subsolar point than the satellites, but may also point to a transient enhancement in solar wind and sheath densities associated with the event. However, we also note that the drop in pressure seen within the magnetosphere is by a factor of $(1.8/1.3) = 1.4$, and if this were due to a corresponding change in solar wind density, the factor we can ascribe to the effect of spatial variations in the magnetosheath is $(2/1.4) = 1.4$. Given

that the satellites were roughly $9 R_E$ from the subsolar point, we can use the gasdynamic predictions of the sheath density variation to estimate that the relevant field lines were reconnected between roughly 3 and $4 R_E$ from the subsolar point.

The relatively long time taken for the event to reach the satellite implies that the tension force initially acted to oppose the sheath flow. Such an orientation is also consistent with a southern hemisphere reconnection site, with the sheath flow acting to take the newly opened flux tubes southward and toward dawn, but the tension force acting to carry them to the north (and towards dawn). This behavior calls for the IMF to have components $B_z < 0$ with $B_y > 0$ at the time when the event was reconnected.

8.3. Event Dimensions

The two-dimensional reconnection pulse model has been found to be very successful in modeling the ion data in this event, in particular the boundary layer structure. For this model we have no information or assumptions that will enable us to estimate the boundary tangential extent of the event in the direction perpendicular to its motion (see discussion by Lockwood *et al.* [1995]).

The use of the stress balance test identifies the event as a convecting structure and gives us an accurate and proper measurement of the velocity of that structure, V_{dHT} . From this we can compute with more confidence the event dimension in the direction of motion ($\Delta t V_{dHT}$), where Δt is the event duration. In total, including the region of draped magnetospheric field, the event lasted $\Delta t_d = 270$ s, although the satellite is in the open LLBL for $\Delta t_i = 120$ s and in the event core for only $\Delta t_c = 30$ s. The derived boundary tangential velocity of the structure is $V_{dHT} = 170 \text{ km s}^{-1}$, yielding boundary tangential extents in the direction of event motion ($\Delta t V_{dHT}$) of 7.2, 3.2, and $0.8 R_E$, for the total event (including the region of field draping), the region of open flux, and the event core, respectively. Note that these dimensions would have been somewhat larger if the satellites had been closer to the magnetopause.

The maximum angles that the event edges make with the nominal LM plane inferred in section (8.1) are $\omega_{in} \approx 7^\circ$ and $\omega_{out} \approx 13^\circ$ for entering and leaving the event, respectively. If we use a simple cosinusoidal shape for both the leading and trailing edges of the event, we can readily estimate the peak boundary normal extent e of the boundary bulge/indentation beyond the satellite location to be

$$e = (2 \Delta t V_{dHT} / \pi) (\cot \omega_{in} + \cot \omega_{out})^{-1} \quad (7)$$

From the values of ($\Delta t V_{dHT}$) derived above, equation (7) yields e of $0.37 R_E$, $0.15 R_E$, and $0.04 R_E$ for the draping region, the open LLBL intrusion, and the event core, respectively. The dimension of $0.37 R_E$ for the draping region is somewhat smaller than the typical $1 R_E$ reported by Saunders *et al.* [1984b], but we should add to our estimate of e the distance between the satellite location and the magnetopause. The depth of the indentation of the event core past the satellite location of $0.04 R_E$ corresponds to just 260 km. Note that with a dimension of $L = 3.2 R_E$ along the magnetopause but just $e = 0.15 R_E$ in the boundary normal direction, the required indentation of the inner edge of the LLBL is shallow.

We can make a second, independent, estimate of the boundary normal extent of the event core from the nested nature of the signatures at the two satellites, given that they are separated by $\Delta N = 180$ km. The event core is seen over the range of transition parameters τ between 14 and 28.5, and in this

interval the difference between the two simultaneous τ values (derived from the two satellites) is approximately constant and averages $\Delta \tau = 10$ (top panel of Figure 12). Thus we can conclude that over the event core, $\Delta N / \Delta \tau$ is approximately constant and equal to $(180/10) \text{ km}$; the range of τ seen in the event core of (28.5-14) corresponds to a distance of $(28.5-14)(\Delta N / \Delta \tau) \approx 260 \text{ km}$. This agrees well with the value obtained above. The similarity between these two independent estimates gives us considerable confidence in their validity.

We can apply the same technique to estimate the width of the putative RD feature seen at τ between 28.5 and 30. In this range of τ , $\Delta \tau$ averages 8, giving $\Delta N / \Delta \tau \approx (180/8) \text{ km}$. This yields a width of $(180/8) \times (30-28.5) = 34 \text{ km}$. Using the thermal ion speed, we find that the ion gyroradius is 40 km, and thus this feature has a width of about 1 ion gyroradius.

9. Conclusions

The success of the ion model in fitting the observations, in particular the evolution of the population in the event boundary layer, shows that this particular FTE event is caused by the satellite sampling field lines, which show a continuous variation in elapsed time since reconnection, consistent with either the magnetosheath pressure pulse model or the reconnection pulse model. The indentation of the inner edge of the open LLBL, which is required in either model, is found to be shallow, only about $0.15 R_E$ deep in the boundary normal dimension in comparison with an inferred boundary tangential extent in the direction of event motion of $3.2 R_E$. The boundary of the core of the FTE has been shown to be a convecting structure, which stress balance suggests may be a slow shock. On the other hand, the ion model explains the main features of the observed ions in terms of flight times between two RDs with no effects of a slow shock seen. The de Hoffman-Teller velocity of this structure and the event core is different from that of the detected sheath flow, whereas they would be the same for the pressure pulse model. However, this test is not definitive because of the long time taken for the satellite to emerge into the magnetosheath. In addition, the reconnection rate variation shows that the field lines at the event center were indeed reconnected in a pulse. However, this finding still does not prove that the bulge was caused by the reconnection pulse. One particular possibility that needs testing is that the reconnection pulse is itself caused by enhanced magnetosheath pressure, such that the FTE signature is the result of both. There are considerable similarities between the open LLBL structure seen within the FTE and simulations, particularly with the results of hybrid simulations [Lin and Lee, 1993a, b].

The tests of the FTE models devised here have not been conclusive in determining the cause of this particular FTE, even if, on balance, they do provide support for the reconnection pulse model. However, in other cases the tension force on newly opened field lines may be larger, and the sheath flow direction could be sampled sooner after and/or shortly before the FTE event. This method would give a more conclusive application of the tests. We here find that a reconnection pulse was indeed present, but we note that this finding is necessary, but not sufficient, to prove that the pulse was indeed the cause of this FTE.

Acknowledgments. This research was carried out under a grant from the UK Particle Physics and Astronomy Research Council. The authors are also grateful to the following Principal Investigators of the AMPTE mission: David Southwood (UKS magnetometer), Alan Johnstone (UKS ion detector), Götz Paschmann (IRM electron and ion detectors) and Hermann

Lühr (IRM magnetometer). We also thank the staff of the CDHF and WDC at RAL for maintaining and archiving the AMPTE data set and making it readily available, Andrew Fazakerly of MSSL for re-processing the AMPTE ion data, and Julia Wolf for the preparation of this camera-ready copy.

The editor thanks Stanley W. H. Cowley and David G. Sibeck for their assistance in evaluating this paper.

References

- Berchem, J., and C. T. Russell, Flux transfer events on the magnetopause: Spatial distribution and controlling factors, *J. Geophys. Res.*, **89**, 6689-6703, 1984.
- Biernat, H.K., M.F. Heyn, and V.S. Semenov, Unsteady Petschek reconnection, *J. Geophys. Res.*, **92**, 3392-3396, 1987.
- Borodkova, N.L., G.N. Zastenker, and D.G. Sibeck, A case and statistical study of transient magnetic field events at geosynchronous orbit and their solar wind, *J. Geophys. Res.*, **100**, 5643-5656, 1995.
- Bryant, D.A., and S. Riggs, At the edge of the Earth's magnetosphere: A survey by AMPTE UKS, *Philos. Trans. R. Soc. London, Ser. A*, **328**, 43-56, 1989.
- Cowley, S. W. H., The causes of convection in the Earth's magnetosphere: A review of developments during IMS, *Rev. Geophys.*, **20**, 531-565, 1982.
- Cowley, S.W.H., and C.J. Owen, A simple illustrative model of open flux tube motion over the dayside magnetopause, *Planet. Space Sci.*, **37**, 1461, 1989.
- Cowley, S.W.H., M.P. Freeman, M. Lockwood, and M.F. Smith, The ionospheric signature of flux transfer events, in *CLUSTER: Dayside Polar Cusp*, Eur. Space Agency Spec. Publ., ESA SP-330, 105-112, 1991.
- Daly, P. W., M. A. Saunders, R. P. Rijnbeek, N. Scokpe, and C. T. Russell, The distribution of reconnection geometry in flux transfer events using energetic ion, plasma, and magnetic data, *J. Geophys. Res.*, **89**, 3843, 1984.
- Ding, F.G., L.C. Lee, and Z.W. Ma, Different FTE signatures generated by the bursty single X line reconnection and the multiple X line reconnection at the dayside magnetopause, *J. Geophys. Res.*, **96**, 57-66, 1991.
- de Hoffmann, F., and E. Teller, Magneto-hydrodynamic shocks, *Phys. Rev.*, **80**, 692, 1950.
- Elphic, R. C., Observations of flux transfer events: Are FTEs flux ropes, islands, or surface waves?, in *Physics of Magnetic Flux Ropes*, *Geophys. Monogr. Ser.*, vol. 58, edited by C. T. Russell, E. R. Priest, and L. C. Lee, pp. 455-472, AGU, Washington, D. C., 1990.
- Elphic, R.C., and D.J. Southwood, Simultaneous measurements of the magnetopause and flux transfer events at widely separated sites by AMPTE UKS and ISEE 1 and 2, *J. Geophys. Res.*, **92**, 13,666-13,672, 1987.
- Elphic, R. C., M. Lockwood, S. W. H. Cowley, and P. E. Sandholt, Signatures of flux transfer events at the dayside magnetopause and in the ionosphere: Combined ISEE, EISCAT and optical observations, *Geophys. Res. Lett.*, **17**, 2241-2244, 1990.
- Elphic, R.C., W. Baumjohann, C.A. Cattell, H. Lühr, and M.F. Smith, A search for upstream pressure pulses associated with flux transfer events: An AMPTE/ISEE case study, *J. Geophys. Res.*, **99**, 13,521-13,527, 1994.
- Fasel, G.J., L.C. Lee, and R.W. Smith, A mechanism for the multiple brightening of dayside poleward moving auroral forms, *Geophys. Res. Lett.*, **20**, 2247-2250, 1993.
- Fasel, G.J., J.I. Minnow, L.C. Lee, R.W. Smith, and C.S. Deehr, Poleward moving auroral forms: What do we really know about them?, in *Physical Signatures of Magnetospheric Boundary Layer Processes*, NATO ASI Ser. C, vol. 425, edited by J.A. Holtet and A. Egeland, pp. 211-226, Kluwer, Dordrecht, 1994.
- Farrugia, C. J., R. C. Elphic, D. J. Southwood, and S. W. H. Cowley, Field and flow perturbations outside the reconnected field line region in flux transfer events: Theory, *Planet. Space Sci.*, **35**, 227-240, 1987a.
- Farrugia, C. J., D. J. Southwood, S. W. H. Cowley, R. P. Rijnbeek, and P. W. Daly, Two-regime flux transfer events, *Planet. Space Sci.*, **35**, 737, 1987b.
- Farrugia, C. J., R. P. Rijnbeek, M. A. Saunders, D. J. Southwood, D. J. Rodgers, M. F. Smith, C. P. Chaloner, D. S. Hall, P. J. Christiansen, and L. J. C. Woolliscroft, A multi-instrument study of flux transfer event structure, *J. Geophys. Res.*, **93**, 14465-14477, 1988.
- Farrugia, C. J., M. P. Freeman, S. W. H. Cowley, D. J. Southwood, M. Lockwood, and A. Etemadi, Pressure-driven magnetopause motions and attendant response on the ground, *Planet. Space Sci.*, **37**, 589-607, 1989.
- Friis-Christensen, E., M.A. McHenry, C.R. Clauer, and S. Vennerstrom, Ionospheric traveling convection vortices observed near the polar cleft: A triggered response to sudden changes in the solar wind, *Geophys. Res. Lett.*, **15**, 253-256, 1988.
- Fuselier, S., Solar wind He⁺ and H⁺ distributions in the cusp for southward IMF, in *Polar Cap Boundary Phenomena*, NATO ASI Ser. C, vol. 509, edited by J. Moen, A. Egeland, and M. Lockwood, pp. 63-72, Kluwer, Dordrecht, 1998.
- Fuselier, S.A., D.M. Klumpar, and F.G. Shelley, Ion reflection and transmission during reconnection at the Earth's subsolar magnetopause, *Geophys. Res. Lett.*, **18**, 139-142, 1991.
- Fuselier, S., B.J. Anderson, and T.G. Onsager, Electron and ion signatures of field line topology at the low shear magnetopause, *J. Geophys. Res.*, **100**, 11,805-11,814, 1995.
- Glaßmeier, K.-H., Traveling magnetospheric convection twin-vortices: Observations and theory, *Ann. Geophys.*, **10**, 547-565, 1992.
- Glaßmeier, K.-H., M. Hoenisch, and J. Untied, Ground-based and satellite observations of traveling magnetospheric convection twin vortices, *J. Geophys. Res.*, **94**, 2520-2528, 1989.
- Goertz, C.K., E. Neilsen, A. Korth, K.-H. Glaßmeier, C. Haldoupis, P. Hoeg, and D. Hayward, Observations of a possible signature of flux transfer events, *J. Geophys. Res.*, **90**, 4069-4078, 1985.
- Gosling, J.T., M.F. Thomsen, S.J. Bame, R.C. Elphic, and C.T. Russell, Cold ion beams in the low-latitude boundary layer during accelerated flow events, *Geophys. Res. Lett.*, **17**, 2245-2248, 1990a.
- Gosling, J.T., M.F. Thomsen, S.J. Bame, T.G. Onsager, and C.T. Russell, The electron edge of the low-latitude boundary layer during accelerated flow events, *Geophys. Res. Lett.*, **17**, 1833-1836, 1990b.
- Haerendel, G., G. Paschmann, N. Scokpe, H. Rosenbauer, and P. C. Hedgecock, The frontside boundary layer of the magnetopause and the problem of reconnection, *J. Geophys. Res.*, **83**, 3195-3216, 1978.
- Hall, D.S., D.A. Bryant, and C.P. Chaloner, Plasma variations at the dayside magnetopause, in *Proceedings of the 7th ESA Symposium on Rockets and Balloons*, Eur. Space Agency Spec. Publ., ESA SP-229, 299-304, 1985.
- Hapgood, M.A., and D.A. Bryant, Exploring the magnetospheric boundary layer, *Planet. Space Sci.*, **40**, 1431-1459, 1992.
- Hapgood, M.A., and M. Lockwood, Rapid changes in LBL thickness, *Geophys. Res. Lett.*, **22**, 77-80, 1995.
- Heyn, M.F., H.K. Biernat, R.P. Rijnbeek, and V.S. Semenov, The structure of reconnection layers, *J. Plasma Phys.*, **40**(2), 235-252, 1988.
- Hudson, P.D., Discontinuities in an isotropic plasma and their identification in the solar wind, *Planet. Space Sci.*, **18**, 1611-1622, 1970.
- Jacobsen, B., P. E. Sandholt, B. Lybekk, and A. Egeland, Transient auroral events near midday: Relationship with solar wind/magnetosheath plasma and magnetic field conditions, *J. Geophys. Res.*, **96**, 1327-1336, 1991.
- Kavano, H., S. Kokubun, and K. Takahashi, Survey of transient magnetic field events in the dayside magnetosphere, *J. Geophys. Res.*, **97**, 10,677-10,692, 1992.
- Kivelson, M.G., and D.J. Southwood, Ionospheric traveling vortex generation by solar wind buffeting of the magnetosphere, *J. Geophys. Res.*, **96**, 1661-1667, 1991.
- Klumpar, D. M., S. A. Fuselier, and E. G. Shelley, Ion composition measurements within magnetospheric flux transfer events, *Geophys. Res. Lett.*, **17**, 2305-2308, 1990.
- Ku, H.C., and D.G. Sibeck, Internal structure of flux transfer events produced by the onset of merging at a single X line, *J. Geophys. Res.*, **102**, 2243-2260, 1997.
- Ku, H.C., and D.G. Sibeck, The effect of magnetosheath plasma flow on flux transfer events produced by the onset of merging at a single X line, *J. Geophys. Res.*, **103**, 6693-6702, 1998.
- Kuo, H., C.T. Russell, and G. Le, Statistical studies of flux transfer events, *J. Geophys. Res.*, **100**, 3513-3519, 1995.
- Lee, L.C., Magnetic flux transfer at the Earth's magnetopause, in *Solar Wind-Magnetosphere Coupling*, edited by Y. Kamide and J. A. Slavin, pp. 297-314, Terra Sci., Tokyo, 1986.
- Lee, L.C., and Z.F. Fu, A theory of magnetic flux transfer at the Earth's magnetopause, *Geophys. Res. Lett.*, **12**, 105-108, 1985.
- Levy, R., H.E. Petschek, and G.L. Siscoe, Aerodynamic aspects of magnetospheric flow, *AIAA J.*, **2**, 2065, 1964.
- Lin, Y., and L.C. Lee, The structure of reconnection layers in the magnetosphere, *Space Sci. Rev.*, **65**, 59-179, 1993a.
- Lin, Y., and L.C. Lee, Structure of the dayside reconnection layer in resistive MHD and hybrid models, *J. Geophys. Res.*, **98**, 3919-3934, 1993b.
- Liu, Z.X., Z.W. Zhu, F. Li, and Z.Y. Pu, Topology and signatures of a model for flux transfer events based on vortex-induced reconnection, *J. Geophys. Res.*, **97**, 19,351-19,361, 1992.
- Lockwood, M., Flux transfer events at the dayside magnetopause: Transient reconnection or magnetosheath pressure pulses?, *J. Geophys. Res.*, **96**, 5497-5509, 1991.
- Lockwood, M., Ionospheric signatures of pulsed magnetopause reconnection, in *Physical Signatures of Magnetopause Boundary Layer Processes*, NATO ASI Ser. C, vol. 425, edited by J.A. Holtet and A. Egeland, pp. 229-243, Kluwer, Dordrecht, 1994.
- Lockwood, M., The location and characteristics of the reconnection, X line

- deduced from low-altitude satellite and ground-based observations, 1, Theory, *J. Geophys. Res.*, **100**, 21,791-21,802, 1995.
- Lockwood, M., Energy and pitch angle dispersions of LLBL/cusp ions seen at middle altitudes: Predictions by the open magnetosphere model, *Ann. Geophys.*, **15**, 1501-1514, 1997.
- Lockwood, M., and C.J. Davis, An analysis of the accuracy of magnetopause reconnection rate variations deduced from cusp ion dispersion characteristics, *Ann. Geophys.*, **14**, 149-161, 1996a.
- Lockwood, M., and C.J. Davis, On the longitudinal extent of magnetopause reconnection bursts, *Ann. Geophys.*, **14**, 865-878, 1996b.
- Lockwood, M., and M.A. Hapgood, How the magnetopause transition parameter works, *Geophys. Res. Lett.*, **24**, 373-376, 1997.
- Lockwood, M., and J. Moen, Ion populations on open field lines within the low-latitude boundary layer: Theory and observations during a dayside transient event, *Geophys. Res. Lett.*, **23**, 2895-2898, 1996.
- Lockwood, M., and M.F. Smith, Low altitude signatures of the cusp and flux transfer events, *Geophys. Res. Lett.*, **16**, 879-882, 1989.
- Lockwood, M., and M.F. Smith, The variation of reconnection rate at the dayside magnetopause and cusp ion precipitation, *J. Geophys. Res.*, **97**, 14,841-14,847, 1992.
- Lockwood, M., and M.F. Smith, Low- and mid-altitude cusp particle signatures for general magnetopause reconnection rate variations, 1, Theory, *J. Geophys. Res.*, **99**, 8531-8555, 1994.
- Lockwood, M., and M.N. Wild, On the quasi-periodic nature of magnetopause flux transfer events, *J. Geophys. Res.*, **98**, 5935-5940, 1993.
- Lockwood, M., M. F. Smith, C. J. Farrugia, and G. L. Siscoe, Ionospheric ion upwelling in the wake of flux transfer events at the dayside magnetopause, *J. Geophys. Res.*, **93**, 5641-5654, 1988.
- Lockwood, M., P.E. Sandholt, and S.W.H. Cowley, Dayside auroral activity and magnetic flux transfer from the solar wind, *Geophys. Res. Lett.*, **16**, 33-36, 1989a.
- Lockwood, M., P.E. Sandholt, S.W.H. Cowley, and T. Oguti, Interplanetary magnetic field control of dayside auroral activity and the transfer of momentum across the dayside magnetopause, *Planet. Space Sci.*, **37**, 1347, 1989b.
- Lockwood, M., S. W. H. Cowley, P. E. Sandholt, and R. P. Lepping, The ionospheric signatures of flux transfer events and solar wind dynamic pressure changes, *J. Geophys. Res.*, **95**, 17,113-17,135, 1990.
- Lockwood, M., H.C. Carlson, and P.E. Sandholt, The implications of the altitude of transient 630 nm dayside auroral emissions, *J. Geophys. Res.*, **98**, 15,571-15,587, 1993a.
- Lockwood, M., W.F. Denig, A.D. Farmer, V. N. Davda, S.W.H. Cowley, and H. Lühr, Ionospheric signatures of pulsed magnetic reconnection at the Earth's magnetopause, *Nature*, **361**, 424-428, 1993b.
- Lockwood, M., J. Moen, S.W.H. Cowley, A.D. Farmer, U.P. Løvhaug, H. Lühr, and V.N. Davda, Variability of dayside convection and motions of the cusp/cleft aurora, *Geophys. Res. Lett.*, **20**, 1011-1014, 1993c.
- Lockwood, M., S.W.H. Cowley, M.F. Smith, R.P. Rijnbeek, and R.C. Elphic, The contribution of flux transfer events to convection, *Geophys. Res. Lett.*, **22**, 1185-1188, 1995a.
- Lockwood, M., S.W.H. Cowley, P.E. Sandholt, and U.P. Løvhaug, Causes of plasma flow bursts and dayside auroral transients: An evaluation of two models invoking reconnection pulses and changes in the Y component of the magnetosheath field, *J. Geophys. Res.*, **100**, 7613-7626, 1995b.
- Lockwood, M., C.J. Davis, M.F. Smith, T.G. Onsager, and W.F. Denig, The location and characteristics of the reconnection X line deduced from low-altitude satellite and ground-based observations, 2, DMSP and EISCAT radar data, *J. Geophys. Res.*, **100**, 21,803-21,814, 1995c.
- Lockwood, M., S.W.H. Cowley, and T.G. Onsager, Ion acceleration at both the interior and exterior Alfvén waves associated with the magnetopause reconnection site: Signatures in cusp precipitation, *J. Geophys. Res.*, **101**, 21,501-21,515, 1996.
- Lockwood, M., C.J. Davis, T.G. Onsager, and J.A. Scudder, Modeling signatures of pulsed magnetopause reconnection in cusp ion dispersion signatures seen at middle altitudes, *Geophys. Res. Lett.*, **25**, 591-594, 1998.
- Lühr, H., W. Blawert, and H. Todd, The ionospheric plasma flow and current patterns of traveling convection vortices: A case study, *J. Atmos. Terr. Phys.*, **55**, 1717-1727, 1993.
- Lühr, H., M. Lockwood, P.A. Sandholt, T.L. Hansen, and T. Moretto, Multi-instrument ground-based observations of a traveling convection vortex event, *Ann. Geophys.*, **14**, 162-181, 1996.
- Ma, Z.W., A. Otto, and L.C. Lee, Core magnetic field enhancement in single X line, multiple X line, and patchy reconnection, *J. Geophys. Res.*, **99**, 6125-6136, 1994.
- Newell, P.T., and D.G. Sibeck, By fluctuations in the magnetosheath and azimuthal flow velocity transients in the dayside ionosphere, *Geophys. Res. Lett.*, **20**, 1719-1722, 1993a.
- Newell, P.T., and D.G. Sibeck, Upper limits on the contribution of flux transfer events to ionospheric convection, *Geophys. Res. Lett.*, **20**, 2829-2832, 1993b.
- Onsager, T.G., A quantitative model of magnetosheath plasma in the low latitude boundary layer, cusp, and mantle, in *Physical Signatures of Magnetospheric Boundary Layer Processes*, NATO ASI, Ser. C, vol. 425, edited by J.A. Holtet and A. Egeland, pp. 385-400, Kluwer, Dordrecht, 1994.
- Onsager T.G., C.A. Kletzing, J.B. Austin, and H. MacKiernan, Model of magnetosheath plasma in the magnetosphere: Cusp and mantle particles at low-altitudes, *Geophys. Res. Lett.*, **20**, 479-482, 1993.
- Paschmann, G., B.U.Ö. Sonnerup, I. Papamastorakis, N. Sckopke, G. Haerendel, S.J. Bame, J.R. Asbridge, J.T. Gosling, C.T. Russell, and R.C. Elphic, Plasma acceleration at the Earth's magnetopause: Evidence for reconnection, *Nature*, **282**, 243-246, 1979.
- Paschmann, G., G. Haerendel, I. Papamastorakis, N. Sckopke, S. J. Bame, J. T. Gosling, and C.T. Russell, Plasma and magnetic field characteristics of magnetic flux transfer events, *J. Geophys. Res.*, **87**, 2159-2168, 1982.
- Paschmann, G., I. Papamastorakis, W. Baumjohann, N. Sckopke, C.W. Carlson, B.U.Ö. Sonnerup, and H. Lühr, The magnetopause for large magnetic shear: AMPTE/IRM observations, *J. Geophys. Res.*, **91**, 11,099-11,115, 1986.
- Petschek, H.E., Magnetic field annihilation, in *AAS-NASA Symposium of Physics of Solar Flares*, NASA Spec. Publ., SP 50, 425, 1964.
- Phan, T.D., et al., Low-latitude flank magnetosheath, magnetopause and boundary layer for low magnetic shear: Wind observations, *J. Geophys. Res.*, **102**, 19,883-19,895, 1997.
- Pinnock, M., A.S. Rodger, J.R. Dudeney, K.B. Baker, P.T. Newell, R.A. Greenwald, and M.E. Greenspan, Observations of an enhanced convection channel in the cusp ionosphere, *J. Geophys. Res.*, **98**, 3767-3776, 1993.
- Pinnock, M., A.S. Rodger, J.R. Dudeney, F. Rich, and K.B. Baker, High spatial and temporal resolution observations of the ionospheric cusp, *Ann. Geophys.*, **13**, 919-925, 1995.
- Potemra, T.A., L.J. Zanetti, R. Elphinstone, J.S. Murphree, and D.M. Klumppar, The pulsating magnetosphere and flux transfer events, *Geophys. Res. Lett.*, **19**, 1615-1618, 1992.
- Pudovkin, M. I., C.-V. Meister, B. P. Besser, and H. K. Biernat, The effective polytropic index in a magnetised plasma, *J. Geophys. Res.*, **102**, 27,145-27,150, 1997.
- Reiff, P. H., T. W. Hill, and J. L. Burch, Solar wind plasma injection at the dayside magnetospheric cusp, *J. Geophys. Res.*, **82**, 479-491, 1977.
- Rijnbeek, R. P., S. W. H. Cowley, D. J. Southwood, and C. T. Russell, A survey of dayside flux transfer events observed by the ISEE 1 and 2 magnetometers, *J. Geophys. Res.*, **89**, 786-800, 1984.
- Rijnbeek, R. P., C. J. Farrugia, D. J. Southwood, M. W. Dunlop, W. A. C. Mier-Jedrejowicz, C. P. Chaloner, D. S. Hall, and M. F. Smith, A magnetic boundary signature within flux transfer events, *Planet. Space Sci.*, **35**, 871-878, 1987.
- Rijnbeek, R.P., V.S. Semenov, A.A. Shmalts, H.K. Biernat, M.F. Heyn, and B.P. Besser, Time-dependent reconnection in a current sheet with velocity shear, *Planet. Space Sci.*, **39**, 1377-1395, 1991.
- Rosenbauer, H., H. Grünwaldt, M.D. Montgomery, G. Paschmann, and N. Sckopke, HEOS 2 plasma observations in the distant polar magnetosphere: The plasma mantle, *J. Geophys. Res.*, **80**, 2723-2737, 1975.
- Russell, C. T., and R. C. Elphic, Initial ISEE magnetometer results: Magnetopause observations, *Space Sci. Rev.*, **22**, 681-715, 1978.
- Russell, C. T., and R. C. Elphic, ISEE observations of flux transfer events at the dayside magnetopause, *Geophys. Res. Lett.*, **6**, 33-36, 1979.
- Sandholt, P.E., M. Lockwood, W.F. Denig, R.C. Elphic, and S. Leontjev, Dynamical auroral structure in the vicinity of the polar cusp: Multipoint observations during southward and northward IMF, *Ann. Geophys.*, **10**, 483-497, 1992.
- Sanny, J., D.G. Sibeck, C.C. Venturini, and C.T. Russell, A statistical study of transient events in the outer dayside magnetosphere, *J. Geophys. Res.*, **101**, 4939-4952, 1996.
- Saunders, M. A., Recent ISEE observations of the magnetopause and low-latitude boundary layer: A review, *J. Geophys.*, **52**, 190-198, 1983.
- Saunders, M. A., C. T. Russell, and N. Sckopke, A dual-satellite study of spatial properties of FTEs, in *Magnetic Reconnection in Space and Laboratory Plasmas*, *Geophys. Monogr. Ser.*, vol. 30, edited by E.W. Hones Jr., pp. 145-152, AGU, Washington, D. C., 1984a.
- Saunders, M. A., C. T. Russell, and N. Sckopke, Flux transfer events, scale size and interior structure, *Geophys. Res. Lett.*, **11**, 131-134, 1984b.
- Scholer, M., Magnetic flux transfer at the magnetopause based on single X line bursty reconnection, *Geophys. Res. Lett.*, **15**, 291-294, 1988a.

- Scholer, M., Strong core magnetic fields in magnetopause flux transfer events, *Geophys. Res. Lett.*, **15**, 748-751, 1988b.
- Scholer, M., Asymmetric time-dependent and stationary magnetic reconnection at the dayside magnetopause, *J. Geophys. Res.*, **94**, 15,099-15,111, 1989.
- Scholer, M., D. Hovestadt, F.M. Ipavich, and G. Gloeckler, Energetic protons, alpha particles and electrons in magnetic flux transfer events, *J. Geophys. Res.*, **87**, 2169, 1982.
- Scokopke, N., G. Paschmann, G. Haerendel, B.U.Ö. Sonnerup, S.J. Bame, T.G. Forbes, E.W. Hones Jr., and C.T. Russell, Structure of the low-latitude boundary layer, *J. Geophys. Res.*, **86**, 2099-2110, 1981.
- Semenov, V.S., I.V. Kubyshkin, H.K. Biernat, M.F. Heyn, R.P. Rijnbeek, B.P. Besser, and C.J. Farrugia, Flux transfer events interpreted in terms of a generalized model for Petschek-type reconnection, *Adv. Space Res.*, **11**(9), 25-28, 1991.
- Semenov, V.S., I.V. Kubyshkin, V.V. Lebedeva, R.P. Rijnbeek, M.F. Heyn, H.K. Biernat, and C.J. Farrugia, A comparison and review of steady-state and time-varying reconnection, *Planet. Space Sci.*, **40**, 63-87, 1992a.
- Semenov, V.S., I.V. Kubyshkin, V.V. Lebedeva, M.V. Sidneva, H.K. Biernat, M.F. Heyn, B.P. Besser, and R.P. Rijnbeek, Time-dependent localized reconnection of skewed magnetic fields, *J. Geophys. Res.*, **97**, 4251-4263, 1992b.
- Semenov, V.S., V.V. Lebedeva, H.K. Biernat, M.F. Heyn, R.P. Rijnbeek, and C.J. Farrugia, Time-varying reconnection: Implications for magnetopause reconnection, *J. Geophys. Res.*, **100**, 21,779-21,789, 1995.
- Shi, Y., C.C. Wu, and L.K.C. Lee, Magnetic field reconnection patterns at the dayside magnetopause: An MHD simulation study, *J. Geophys. Res.*, **96**, 17,627-17,650, 1991.
- Sibeck, D. G., A model for the transient magnetospheric response to sudden solar wind dynamic pressure variations, *J. Geophys. Res.*, **95**, 3755-3771, 1990.
- Sibeck, D.G., Transient events in the outer magnetosphere: Boundary waves or flux transfer events?, *J. Geophys. Res.*, **97**, 4009-4026, 1992.
- Sibeck, D.G., Magnetosheath magnetic field variability, *Adv. Space Res.*, **14**(7), 91-94, 1994.
- Sibeck, D.G., and D.G. Croley Jr., Solar wind dynamic pressure variations and possible ground signatures of flux transfer events, *J. Geophys. Res.*, **96**, 1669-1683, 1991.
- Sibeck, D.G., and P.T. Newell, Pressure-pulse driven surface waves at the magnetopause: a rebuttal, *J. Geophys. Res.*, **100**, 21,773-21,778, 1995.
- Sibeck, D.G., and M.F. Smith, Magnetospheric plasma flows associated with boundary waves and flux transfer events, *Geophys. Res. Lett.*, **19**, 1903-1906, 1992.
- Sibeck, D.G., et al., The magnetospheric response to 8-minute period strong-amplitude upstream pressure variations, *J. Geophys. Res.*, **94**, 2505-2519, 1989a.
- Sibeck, D. G., W. Baumjohann, and R. E. Lopez, Solar wind dynamic variations and transient magnetospheric signatures, *Geophys. Res. Lett.*, **16**, 13-16, 1989b.
- Smith, M.F., and C.J. Owen, Temperature anisotropies in a magnetospheric FTE, *Geophys. Res. Lett.*, **19**, 1907-1910, 1992.
- Smith, M.F., and D. J. Rodgers, Ion distributions at the dayside magnetopause, *J. Geophys. Res.*, **96**, 11,617-11,624, 1991.
- Smith, M.F., D.J. Rodgers, and M.A. Saunders, Ion flows in magnetospheric flux transfer events, in *Proceedings of the 21st ESLAB Symposium at Bolkesjø, Eur. Space Agency Spec. Publ. ESA SP-275*, 153-158, 1987.
- Song, P., G. Le, and C.T. Russell, Observational differences between flux transfer events and surface waves at the magnetopause, *J. Geophys. Res.*, **99**, 2309-2320, 1994.
- Sonnerup, B.U.Ö., G. Paschmann, I. Papamastorakis, N. Scokopke, G. Haerendel, S.J. Bame, J.R. Ashbridge, J.T. Gosling, and C.T. Russell, Evidence for magnetic field reconnection at the Earth's magnetopause, *J. Geophys. Res.*, **86**, 10,049-10,067, 1981.
- Sonnerup, B.U.Ö., I. Papamastorakis, G. Paschmann, and H. Lüth, The magnetopause for large magnetic shear: Analysis of convection electric fields from AMPTE/IRM, *J. Geophys. Res.*, **95**, 10,541-10,557, 1986.
- Southwood, D. J., Theoretical aspects of ionosphere-magnetosphere-solar wind coupling, *Adv. Space Res.*, **5**(4), 7-14, 1985.
- Southwood, D. J., The ionospheric signature of flux transfer events, *J. Geophys. Res.*, **92**, 3207-3213, 1987.
- Southwood, D. J., M. A. Saunders, M. W. Dunlop, W. A. C. Mier-Jedrzejowicz, and R. P. Rijnbeek, A survey of flux transfer events recorded by UKS spacecraft magnetometer, *Planet. Space Sci.*, **34**, 1349-1359, 1986.
- Southwood, D. J., C. J. Farrugia, and M. A. Saunders, What are flux transfer events?, *Planet. Space Sci.*, **36**, 503-508, 1988.
- Spreiter, J.R., A.L. Summers, and A.Y. Alksne, Hydromagnetic flow around the magnetosphere, *Planet. Space Sci.*, **14**, 223-253, 1966.
- Thompson, M., J. A. Stansberry, S. J. Barne, S. A. Fuselier, and J. T. Gosling, Ion and electron velocity distributions within flux transfer events, *J. Geophys. Res.*, **92**, 12,127, 1987.
- Todd, H., B.J.I. Bromage, S.W.H. Cowley, M. Lockwood, A.P. van Eyken, and D.M. Willis, EISCAT observations of bursts of rapid flow in the high latitude dayside ionosphere, *Geophys. Res. Lett.*, **13**, 909-912, 1986.
- Walthour, D.W., B.U.Ö. Sonnerup, R.C. Elphic, and C.T. Russell, Double vision: Remote sensing of a flux event, *J. Geophys. Res.*, **99**, 8555-8563, 1994.

M. A. Hapgood and M. Lockwood, Space Science Department, Rutherford Appleton Laboratory, Chilton, Didcot, Oxfordshire OX11 0QX, England, U. K. (email: M.Lockwood@rl.ac.uk and M.Hapgood@rl.ac.uk)

(Received December 31, 1997; revised April 16, 1998; accepted June 6, 1998.)